Development 140, 751-764 (2013) doi:10.1242/dev.090159

Spatiotemporal patterns of multipotentiality in *Ptf1a*-expressing cells during pancreas organogenesis and injury-induced facultative restoration

Fong Cheng Pan[1], Eric D. Bankaitis[1], Daniel Boyer[1], Xiaobo Xu[2], Mark Van de Casteele[3], Mark A. Magnuson[4], Harry Heimberg[3] and Christopher V. E. Wright[1,*]

SUMMARY

Pancreatic multipotent progenitor cells (MPCs) produce acinar, endocrine and duct cells during organogenesis, but their existence and location in the mature organ remain contentious. We used inducible lineage-tracing from the MPC-instructive gene *Ptf1a* to define systematically in mice the switch of Ptf1a$^+$ MPCs to unipotent proacinar competence during the secondary transition, their rapid decline during organogenesis, and absence from the mature organ. Between E11.5 and E15.5, we describe tip epithelium heterogeneity, suggesting that putative Ptf1a$^+$Sox9$^+$Hnf1β$^+$ MPCs are intermingled with Ptf1a^{HI}Sox9^{LO} proacinar progenitors. In the adult, pancreatic duct ligation (PDL) caused facultative reactivation of multipotency factors (Sox9 and Hnf1β) in Ptf1a$^+$ acini, which undergo rapid reprogramming to duct cells and longer-term reprogramming to endocrine cells, including insulin$^+$ β-cells that are mature by the criteria of producing Pdx1^{HI}, Nkx6.1$^+$ and MafA$^+$. These Ptf1a lineage-derived endocrine/β-cells are likely formed via Ck19$^+$/Hnf1β$^+$/Sox9$^+$ ductal and Ngn3$^+$ endocrine progenitor intermediates. Acinar to endocrine/β-cell transdifferentiation was enhanced by combining PDL with pharmacological elimination of pre-existing β-cells. Thus, we show that acinar cells, without exogenously introduced factors, can regain aspects of embryonic multipotentiality under injury, and convert into mature β-cells.

KEY WORDS: Multipotent pancreas progenitors, Facultative progenitors, Acinar-to-endocrine transdifferentiation, Injury, Mouse, Lineage tracing

INTRODUCTION

The inherent plasticity potential of adult pancreas is especially interesting considering the possibility of controllably reprogramming various cell types into β-cells as an alternative to embryonic stem cell differentiation and transplantation therapy for diabetes. Pancreatic multipotent progenitor cells (MPCs) are the basis for generating a functional pancreas with appropriate cell allocations and structures. Understanding the ontogeny and intermediate states of MPCs could provide insight into whether the differentiated adult pancreatic cells could be challenged to return to an embryonic multipotency under stimuli such as physiological injury or chronic diabetes.

The early pancreatic epithelium contains MPCs producing several transcription factors (TFs), including Ptf1a, associated with commitment toward pancreatic fate, and controlling early organ growth (Pan and Wright, 2011). At the beginning of morphogenetic maturation [around embryonic day (E) 12], the epithelium becomes compartmentalized into 'tip' and 'trunk' domains (Zhou et al., 2007; Villasenor et al., 2010). Genetic lineage-tracing via *Cpa1*^{CreER} suggested that MPCs with the rudimentary signature Pdx1$^+$Ptf1a$^+$cMyc^{High}CpaI$^+$ are located at the tip domain, but rapidly disappear with the start of the secondary (2°) transition (Zhou et al., 2007), and the trunk epithelium between E12.5 and E15.5 was proposed to harbor bipotential progenitor pools for duct and endocrine cells (Zhou et al., 2007; Schaffer et al., 2010). Lineage-tracing analysis using *Hnf1β*^{CreER} (Solar et al., 2009) and *Sox9*^{CreER} (Kopp et al., 2011), however, suggested that trunk epithelium contains a progressively reducing number of MPCs, even after overt tip-trunk segregation. While the Hnf1β$^+$ population is multipotent during the early 2° transition, but largely bipotential at later stages, relatively low numbers of Sox9$^+$ cells were proposed to feed all pancreatic lineages throughout embryogenesis, suggesting persistence of Sox9$^+$ MPCs after the 2° transition (Kopp et al., 2011). Because Sox9$^+$ and Hnf1β$^+$ cells were localized to the trunk epithelium, with CpaI$^+$ cells at the tips, the precise location and number, and molecular signature, of MPCs during and after the 2° transition remains unclear.

The existence of adult facultative progenitors capable of regenerating endocrine cells under special stimuli has been contentious (Granger and Kushner, 2009). Recent lineage tracing in mice, however, yielded the surprising suggestion that many terminally differentiated cell types could be reprogrammed to other cell-types, either using exogenous factors or under injury conditions. Xu et al. (Xu et al., 2008) concluded that facultative Ngn3$^+$ (Neurog3$^+$ – Mouse Genome Informatics) endocrine progenitors, producing β-cells *ex vivo*, appeared in/at the duct following pancreatic duct ligation (PDL). By contrast, lineage-tracing results with duct/centroacinar-specific CreER lines (*Hnf1β*^{CreER}, *Hes1*^{CreER}, *Sox9*^{CreER}) provided evidence against duct and centroacinar cells deriving endocrine cells after PDL (Solar et al., 2009; Kopinke et al., 2011; Furuyama et al., 2011; Kopp et al., 2011). Detailed studies are required to determine rigorously the origin of the Ngn3$^+$ duct cells and if they progress to islet/β-cells *in vivo*.

[1]Vanderbilt University Program in Developmental Biology, Department of Cell and Developmental Biology, Vanderbilt University Medical Center, Nashville, TN 37232, USA. [2]Department of Medicine, Childrens Hospital Boston, Harvard Medical School, 300 Longwood Avenue, Enders 922, Boston, MA 02115, USA. [3]Diabetes Research Center, Vrije Universiteit Brussels, Laarbeeklaan 103 D2, Brussels, B1090 Belgium. [4]Vanderbilt University Center for Stem Cell Biology, 9465 MRB IV, 2213 Garland Avenue, Nashville, TN 37232-0494, USA.

*Author for correspondence (chris.wright@vanderbilt.edu)

Accepted 3 December 2012

Because of their vast number, acinar cells could be an attractive source for replenishing β-cells to offset losses from disease or injury. Acinar-to-endocrine conversion was suggested with primary acinar cells cultured *in vitro* when treated with growth factors (Baeyens et al., 2005; Minami et al., 2005). *In vivo* lineage-tracing using *Elastase*^{CreER}, however, showed no evidence of such conversion upon regeneration/injury with partial pancreatectomy (Ppx), PDL, or cerulein-induced pancreatitis (Desai et al., 2007). Strikingly, overexpression of three β-cell TFs – Pdx1, Ngn3, MafA – apparently turned acini into β-like cells *in vivo*, suggesting convertibility under strong stimuli (Zhou et al., 2008). It remains unclear whether all acinar cells are equally susceptible to such conversion, and if it could be activated without genetic intervention or under injury conditions that might exist in diabetes or pancreatitis.

Ptf1a is expressed in early bud MPCs, with an instructive role in distinguishing pancreatic fate from the adjacent organs (Kawaguchi et al., 2002). In the 2° transition pancreatic epithelium, Ptf1a production is dynamically regulated. Over time, its activity changes from driving an MPC program to directing tip cells into a proacinar state. Moving from MPC to proacinar behavior is proposed to be linked to the switching of Ptf1a co-regulatory proteins in the trimeric PTF1 complex, from PTF1$^{RBP\text{-}J}$ to PTF1$^{RBP\text{-}JL}$ (Masui et al., 2007). An outstanding issue is whether small numbers of Ptf1a$^+$ MPCs persist during/after the 2° transition, or if adult Ptf1a$^+$ acini could somehow re-engage (aspects of) an embryonic Ptf1a-driven MPC program, to adopt facultative progenitor activity.

Here, we report a knock-in tamoxifen-inducible *Ptf1a*^{CreERTM} line for the dissection of gene regulatory networks critical for maintaining the MPC state and controlling tip-trunk compartmentalization. We reasoned that lineage-tracing analysis performed using the MPC-instructive factor Ptf1a would provide more certainty in addressing the intrinsic potentiality (mono, bi, or multi) of pancreatic progenitor populations during organogenesis. We describe a dynamic heterogeneity within the tip epithelium, based on distinct TF signatures, which changes during tip-trunk segregation concordant with the shift from multipotency to unipotency in *Ptf1a*-expressing cells. Pulse-labeling-type lineage-tracing using *Ptf1a*^{CreERTM} showed that the number of Ptf1a$^+$ MPCs decreased progressively and rapidly during organogenesis, with rare MPCs present late into the 2° transition, and perinatal/adult stage *Ptf1a*$^+$ cells produce only acinar cells. However, *Ptf1a*$^+$ acinar cells were activated by PDL to become facultative progenitors, express several embryonic multipotency factors and become competent to produce duct and endocrine cells, including mature β-cells. Acinar-to-endocrine conversion was detected in substantial numbers only 2 months post-PDL, but their formation was enhanced by eliminating pre-existing β-cells with a selective toxin, streptozotocin (STZ). This is the first study to demonstrate, with *in vivo* lineage-tracing, that acinar cells give rise to endocrine cells under injury-induced reprogramming paradigms and without additional transcription factors or signaling molecules.

MATERIALS AND METHODS

Mice

Ptf1a^{CreERTM} was generated using recombinase-mediated cassette exchange (Long et al., 2004) (supplementary material Fig. S1A). *R26R*^{lacZ} and *R26R*^{EYFP} mice were described previously (Soriano, 1999; Srinivas et al., 2001). Animals and embryos were PCR-genotyped. Experiments were under protocols approved by Vanderbilt University IACUC.

Tamoxifen administration and injury procedures

Tamoxifen (Tam, Sigma T-5648) was 30 mg/ml in corn oil (Sigma C8267). Tamoxifen administration and dosage used were described in detail in results section. PDL was performed as described (Xu et al., 2008). Streptozotocin (STZ; 10 mg/ml in sodium citrate pH 4.5) was given intraperitoneally (100 mg/kg) for 2 consecutive days at post-PDL D3.

Tissue preparation and immunostaining

Embryonic or adult pancreas was fixed (2-4 hours, 4% paraformaldehyde, 4°C), and for cryosections, washed twice in cold PBS, sucrose-equilibrated (30%, 4°C, overnight), and embedded in OCT compound (Tissue-Tek, Sakura). Paraffin sections, whole-mount β-galactosidase detection, H&E staining, processing was as described (Kawaguchi et al., 2002). Immunofluorescence used 10 μm cryosections (Kawaguchi et al., 2002). Antibodies used are listed in supplementary material Table S1.

Data collection, morphometric and statistical analysis

Images from Zeiss confocal (LSM 510 META upright) or Apotome were analyzed with LSM Image Browser and Zeiss Axiovision 4.8 software, respectively. Systematic quantitation analysis was performed by Photoshop CS3 and NIH ImageJ software.

Short-term lineage tracing, E13.5 and E14.5: labeling of the acini, ducts or endocrine cells was manually scored as percentage of each EYFP$^+$ cell-type of total cell number in each compartment, using all field of view, every other section (20 μm apart; ~50% total pancreas). E18: every sixth section (60 μm apart, ~16% total pancreas) was counted. Juvenile/adult mice: 150-200 random fields from 40 evenly spaced sections (100 μm apart; ~10% of total pancreas) were analyzed. For E18.5, and juvenile/adult pancreata, percentage labeling was calculated based on EYFP$^+$ area over total area for each cell type. Head/tail pieces of PDL pancreata were separately embedded and analyzed. All fields of view from every 100 μm section (~40-45; ~10% total pancreas) ensured coverage of all regions. At least three to four pancreata per stage/group were analyzed. Two-tailed Student's *t*-test used a significance of $P<0.05$.

RESULTS

Generation and characterization of *Ptf1a*^{CreERTM} mice

Given that *Ptf1a* is expressed in early pancreatic MPCs (Kawaguchi et al., 2002), and later at E12 is seemingly restricted to MPC/proacinar progenitors in the tip epithelium of the remodeling epithelial plexus (Zhou et al., 2007), it was critical to determine quantitatively the dynamics of this shift from multipotential to unipotential behavior. To lineage-trace *Ptf1a*-expressing cells at different stages of pancreas organogenesis, we derived *Ptf1a*^{CreERTM} knock-in mice expressing CreER^{TM} under endogenous *Ptf1a* promoter/enhancer elements (supplementary material Fig. S1A). CreER^{TM} production recapitulates endogenous *Ptf1a* expression, with nuclear translocation induced in Ptf1a$^+$ and CpaI$^+$ acinar cells within 24 hours of tamoxifen (Tam) administration at E15.5 (supplementary material Fig. S2A,B).

Testing *Ptf1a*^{CreERTM} mice with reporter alleles (*Rosa26R*^{lacZ} [*R26R*^{lacZ}] or *Rosa26R*^{EYFP} [*R26R*^{EYFP}]) and Tam administered at designated developmental stages allowed indelible marking of the progeny of *Ptf1a*$^+$ cells throughout subsequent development. Recombination of *R26R*^{lacZ} was strictly tamoxifen-dependent and no pancreatic β-gal$^+$ cells were detected in non-CreER^{TM} mice (supplementary material Fig. S3A,B; Fig. 1C,C′). For embryonic labeling, while single 3 mg Tam doses at E16.5 and E18.5 resulted in ~50-60% labeling of acinar cells (supplementary material Fig. S3D; Fig. 3B-D), lower labeling (~10-40%) occurred with single 3 mg Tam doses at earlier stages (E9.5-13.5; Fig. 1D″,E″,F″,G″). For adults, three 3 mg Tam doses over 6 days resulted in ~60-80% recombination of *R26R*^{lacZ} or *R26R*^{EYFP} (supplementary material Fig. S3B; Fig. 3E-J). *Ptf1a*^{CreERTM}-induced *R26R*^{lacZ} recombination

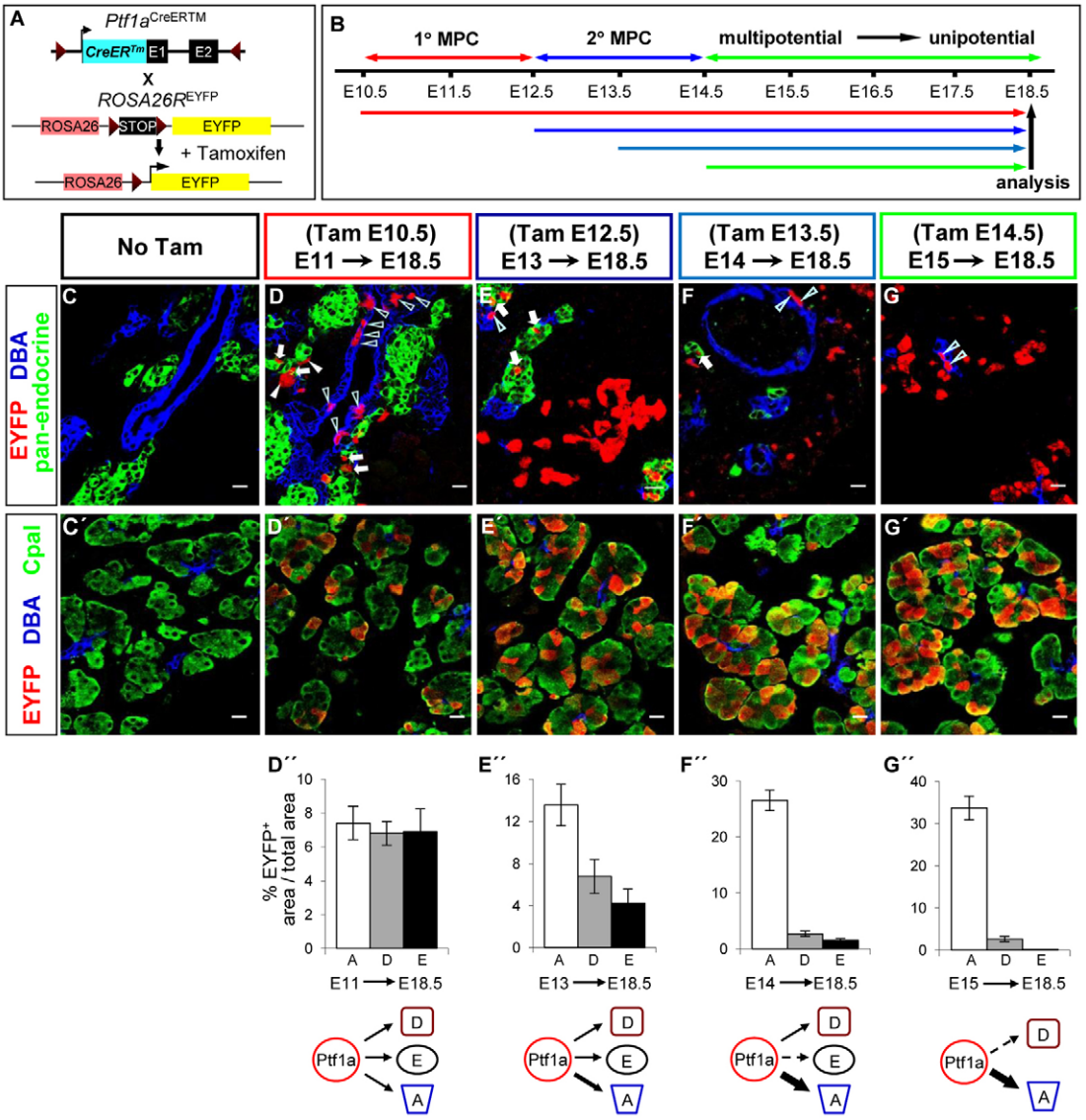

Fig. 1. Lineage tracing *Ptf1a*-expressing cells. (**A**) Tam-dependent *Ptf1a*^{CreERTM} recombination of *R26R*^{EYFP} irreversibly labels *Ptf1a*-expressing cells and progeny. (**B**) Color-coded E10.5-15.5 lineage-tracing scheme. (**C**,**C′**) *Ptf1a*^{CreERTM} recombination is strictly Tam-dependent. (**D-F′**) *Ptf1a*-expressing cells pulse-labeled at (D,D′) E11, (E,E′) E13 or (F,F′) E14 produced endocrine, duct and acinar cells in various proportions (arrow: EYFP$^+$ endocrine$^+$ cells; open arrowhead: EYFP$^+$DBA$^+$ duct cells). (**G**,**G′**) E15 labeling produced acini and small numbers of duct cells. (**D″-G″**) Histogram representation of EYFP$^+$ cells in (A, acinar; D, duct; E, endocrine) compartments after Tam labeling at E11 (D″; *n*=4), E13 (E″; *n*=3), E14 (F″; *n*=5), and E15 (G″; *n*=3). Quantitation is total EYFP$^+$ area of each cell type over total area of each cell type. Scale bars: 20 μm.

in adult pancreas was Tam-dose-dependent; labeling efficiency was enhanced moving from 1 to 3 mg (supplementary material Fig. S3C). *Ptf1a*^{CreERTM} is therefore valuable for pulsed-labeling studies, and conditional inactivation of genes involved in pancreas development/cancer, with excellent spatiotemporal control.

Early *Ptf1a*-expressing cells contribute to all three pancreatic lineages

Ptf1a^{CreERTM};*R26R*$^{EYFP/EYFP}$ embryos were generated at various stages (Fig. 1A). Single 3 mg Tam dosing of *Ptf1a*^{CreERTM};*R26R*^{EYFP} pregnant mice at E10.5 would label *Ptf1a*-expressing cells of the primary (1°) transition (E9.5-12); pulses between E12.5-14.5 would label 2° transition *Ptf1a*-expressing cells; and at E15.5 or later would test whether *Ptf1a*-expressing cells had completely switched from multipotential behavior (Fig. 1B). Pancreata were analyzed near the end of gestation (E18.5) for co-localization of EYFP (derivation from *Ptf1a*$^+$ cells) with endocrine, ductal and acinar markers. The percentage of labeled (EYFP$^+$) cells expressing each marker was quantified by a strategy taking into account the potential variation in proliferation and cell sizes in the acinar, duct or endocrine compartment. Because nuclear CreER localization starts ~6-12 hours post-Tam-injection with a 36-hour end point (supplementary material Fig. S2) (Ahn and Joyner, 2004; Danielian et al., 1998), data are presented as each injection point having a labeling period offset by 12-36 hours.

Tam pulses at E10.5 (E11 labeling; *n*=4) labeled EYFP$^+$ cells equivalently in all three epithelium-derived compartments – acini/duct/endocrine – indicating that the Ptf1a$^+$ population is multipotent at this stage (Fig. 1D,D′), and consistent with previous studies showing Ptf1a marks early pancreatic bud MPCs (Kawaguchi

et al., 2002; Burlison et al., 2008). The percentage of EYFP$^+$ cells per compartment was reproducibly comparable (Fig. 1D″; supplementary material Fig. S1B), suggesting that the early MPC population contributes equally to all three lineages, including all endocrine cell types (supplementary material Fig. S1F).

Ptf1a$^+$ MPC numbers decrease dramatically during the 2° transition

To determine the degree to which the Ptf1a$^+$ population maintains multipotency over the 2° transition (E12.5-15.5), single Tam doses were given at E12.5, E13.5 and E14.5, with analysis at E18.5. Labeling at E13 and E14 yielded lineage-traced endocrine, duct and acinar cells (Fig. 1E,E′,F,F′), indicating that significant numbers of Ptf1a$^+$ MPCs exist during the 2° transition. Quantitation showed a tendency to produce acinar over duct and endocrine cells (E13, *n*=3; E14, *n*=5; Fig. 1E,F; supplementary material Fig. S1C,D,E). In particular, the E13 result suggests that the tip epithelium at this stage already contains different populations of *Ptf1a*-expressing cells, in accordance with immuno-colocalization data below. These findings largely agree with *CpaI*^{CreERT2} studies demonstrating diminution of the MPC pool during the 2° transition (Zhou et al., 2007). With labeling at E15, lineage-trace was predominantly restricted to acini and to a much lesser extent duct cells (*n*=3; Fig. 1G-G″). Taken together, these data indicate that *Ptf1a*-expressing cells have almost completely switched to unipotential acinar progenitor behavior by ~E15, with a minimal late-stage-remaining contribution to the duct compartment.

Shorter-term lineage-tracing was performed to assess lineage allocation of *Ptf1a*-expressing MPCs during the 2° transition, specifically to determine the extent to which tip MPC yield progeny moving into the trunk epithelium (the presumptive location of the endocrine/duct bipotent pool). Twenty-four hours post-labeling (injecting at E12.5, E13.5; analyzing at E13.5 or E14.5), numerous CpaI$^+$ proacinar/acinar cells were EYFP$^+$ (of total CpaI$^+$ tip cells: ~8.3±3.2% at E13.5, ~11.3±2.70% at E14.5; *n*=4; Fig. 2B,E,F,I). EYFP$^+$Hnf1β$^+$ cells in trunk epithelium were also regularly observed but at a relatively low frequency (of total Hnf1β$^+$ trunk cells: ~2.1±0.9% at E13.5, ~1.5±0.9% at E14.5; *n*=4; Fig. 2D,E,H,I). Therefore, *Ptf1a*-lineage cells could contribute to both tip, and to a lesser extent, trunk compartments at ~E13/14, the stage of progression into the secondary transition proper. EYFP$^+$Ngn3$^+$ endocrine progenitors and EYFP$^+$Synaptophysin$^+$ endocrine cells (synaptophysin labels endocrine precursors and differentiated hormone$^+$ cells), although rare in number, were found 24 hours post-labeling [of total (Ngn3$^+$+Synaptophysin$^+$) cells: 0.2±0.1% at E13.5, ~0.06±0.04% at E14.5; *n*=4; Fig. 2C,E,G,I]. These analyses provide direct evidence, consistent with the longer-term tracing above, that the *Ptf1a*-expressing tip population is already undergoing, near the initiation of the 2° transition, significant restriction of lineage multipotency. We next questioned to what extent the *Ptf1a*-expressing tip domain comprised heterogeneous populations of qualitatively distinct cell-types, based on their production of TFs associated with multipotency.

2° transition tip epithelium heterogeneity: putative Ptf1a$^+$Sox9$^+$Hnf1β$^+$ MPC versus Ptf1a^{HI}Sox9^{LO}Hnf1β$^-$ proacinar progenitors

We explored the signature of putative Ptf1a$^+$ MPCs between E11.5 and E15.5 to try to move beyond the general signature of Pdx1$^+$Ptf1a$^+$CpaI$^+$cMyc^{HI} proposed by Zhou et al. (Zhou et al., 2007). We monitored co-localization and relative levels of Ptf1a with Sox9 and Hnf1β, two TFs having loss-of-function evidence of important roles in MPC formation (Seymour et al., 2007; Haumaitre et al., 2005). At E11 and E11.75, with the initiation of tip-trunk compartmentalization, the pancreatic epithelium displayed significant heterogeneity, with three populations observable: (1) Ptf1a^{HI}Sox9^{LO} cells located in peripheral regions of the branching bud epithelium; (2) Ptf1a$^-$Sox9$^+$ cells concentrated in the prospective trunk domain; and (3) Ptf1a$^+$Sox9$^+$ cells scattered throughout the epithelium (Fig. 2J,K).

By E12.5, tip and trunk domains were relatively distinct based on Ptf1a and Sox9 production, respectively (Fig. 2L). Between E12.5 and E15.5, Ptf1a$^+$Sox9$^+$ tip cells were found distributed at both tip-trunk interface and intra-tip regions, intermingled with the Ptf1a^{HI}Sox9^{LO} (proacinar) population (Fig. 2L-O; supplementary material Fig. S4A-F). The numbers of these Ptf1a$^+$Sox9$^+$ decreased progressively over this period. Conversely, the Ptf1a^{HI}Sox9^{LO} population increased to comprise the entire tip domain by E15.5. Ptf1a$^+$Sox9$^+$ tip cells were also Hnf1β$^+$ and CpaI$^+$ (supplementary material Fig. S4A-F), and thus may represent the MPCs persisting during the early 2° transition, as marked by our lineage-tracing (Fig. 2P). Notably, the relative signal intensity of Ptf1a, Sox9 and Hnf1β in some of the tip MPC population seems lower compared to the robust signals in the trunk (for Sox9/Hnf1β) or proacini (for Ptf1a). But, determining if lower levels of these co-expressed TFs are necessarily associated with MPC character awaits future tools that allow isolation of this population. Our co-expression and lineage-tracing data fit the notion that multipotent Ptf1a$^+$ tip populations diminish rapidly during the 2° transition as they convert to Ptf1a^{HI} proacinar cells.

Ptf1a$^+$ cells produce only acini after birth

From birth until weaning, islet cell mass increases parallel to body mass in mouse and rat (Bouwens and Rooman, 2005). We found no evidence that endocrine cells arise from *Ptf1a*-expressing cells during this endocrine expansion period. Single 3 mg Tam doses were given to *Ptf1a*^{CreERTM};*R26R*^{EYFP} pregnant mice near the end of gestation (E18.5) and pancreata were analyzed at postnatal day 21 (P21; *n*=4; Fig. 3A). EYFP was found exclusively in CpaI$^+$ acinar cells (Fig. 3B-D), suggesting that postnatal *Ptf1a*-expressing cells contribute to neither endocrine nor duct compartments.

To determine if duct or endocrine cells arise from Ptf1a$^+$ cells during normal homeostasis in young adults, we treated P30 mice with three doses of Tam (Fig. 3A). Two days after the last injection (P36), a high proportion of acinar cells were labeled (60.9±3.83%; *n*=4; Fig. 3E-G), increasing to 72.6±5.39% after 6 months post-Tam. No EYFP$^+$ cells were found in the duct or endocrine compartments at either age (P36, 7-month; *n*=4; Fig. 3H-J). We also failed to detect Hnf1β$^+$Ck19$^+$ (Ck19 is also known as Krt19 – Mouse Genome Informatics) centroacinar cells (CACs) labeled with EYFP after 6-month chase (Fig. 3K,K′,L,M), consistent with a lack of Ptf1a immunoreactivity in Sox9$^+$Ck19$^+$ and Hnf1β$^+$Ck19$^+$ CACs (Fig. 3M-M‴; supplementary material Fig. S6A). These latter results suggest that *Ptf1a* expression does not mark CACs *in vivo*, contrasting a previous study reporting *Ptf1a* expression in flow-sorted CACs (Rovira et al., 2010). Together, these data suggest that Ptf1a$^+$ cells self-replicate to maintain the acinar pool in the adult organ, with no contribution towards the duct or endocrine populations.

PDL induces ductal transdifferentiation of Ptf1a$^+$ acinar cells, reactivating MPCs and endocrine progenitor factors

We endeavored to determine whether *Ptf1a*-expressing acinar cells could exhibit facultative progenitor activity under PDL, exhibiting

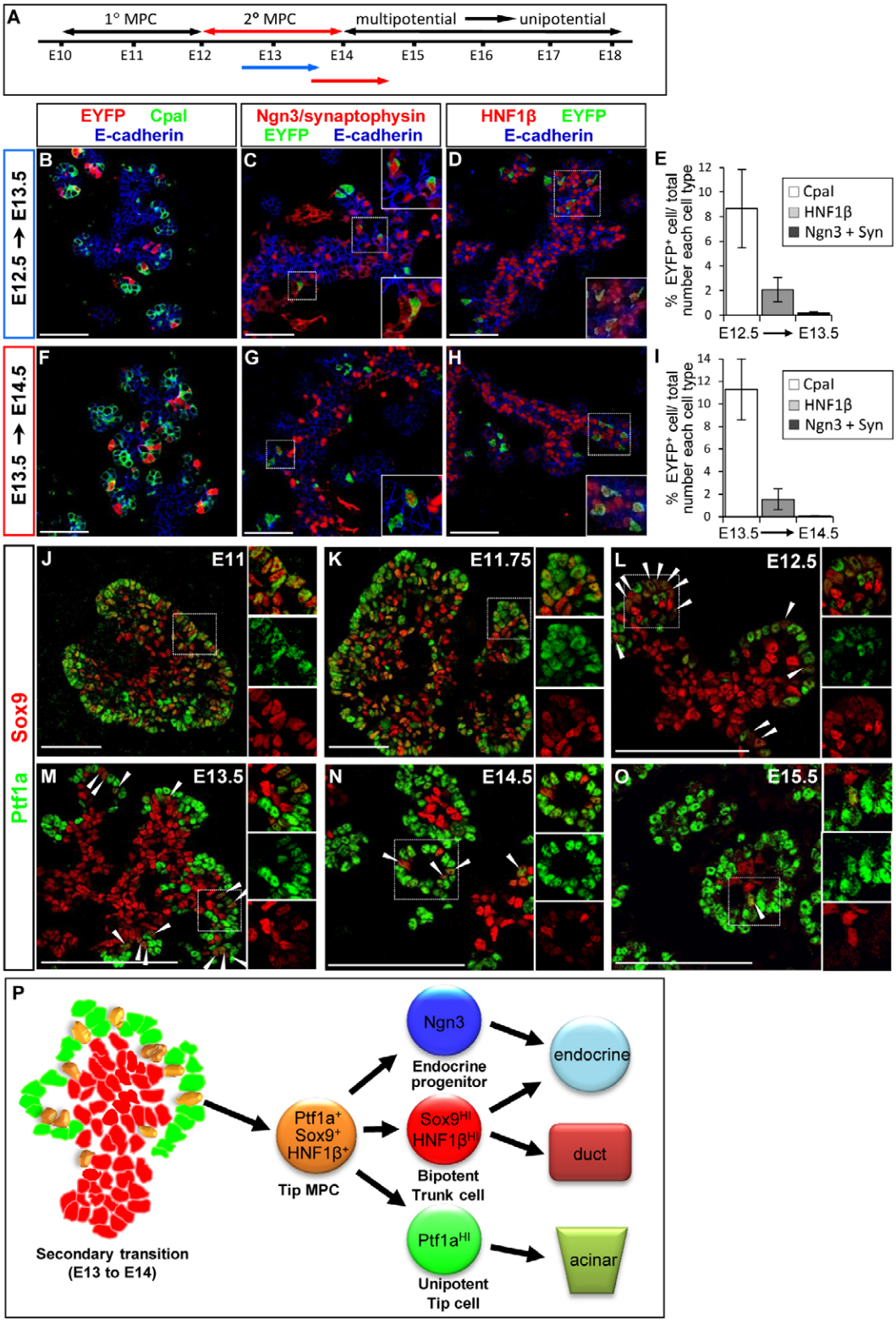

Fig. 2. Ptf1a^{+} tip cell contribution to trunk and endocrine progenitor/precursor compartment, and heterogeneity in 2°-transition tip epithelium (with putative Ptf1a^{LO} MPC and Ptf1a^{HI} proacinar cells). (**A**) Short-term lineage-tracing schematic. (**B-D**,**F-H**) EYFP-labeled CpaI^{+} tip cells, Hnf1β^{+} trunk cells, and Ngn3^{+}/Synaptophysin^{+} (Syn) endocrine precursors were detected 24 hours post-labeling of *Ptf1a*-expressing cells at (B-D) E12.5 or (F-H) E13.5. (**E**,**I**) Percentage EYFP^{+} cells in each lineage with labeling at E12.5 (E; *n*=4) or E13.5 (I; *n*=4). (**J-O**) Ptf1a/Sox9 immunodetection between E11-15.5 showing tip epithelium with two Ptf1a^{+} populations: Ptf1a^{+}Sox9^{+} putative MPC (arrowhead), and Ptf1a^{HI}Sox9^{LO} proacinar progenitors. Numbers of Ptf1a^{+}Sox9^{+} cells decreased rapidly as organogenesis progressed. (**P**) Schematic, lineage potency of Ptf1a^{+}Sox9^{+}Hnf1β^{+} tip MPC during the 2° transition. Scale bars: 50 μm.

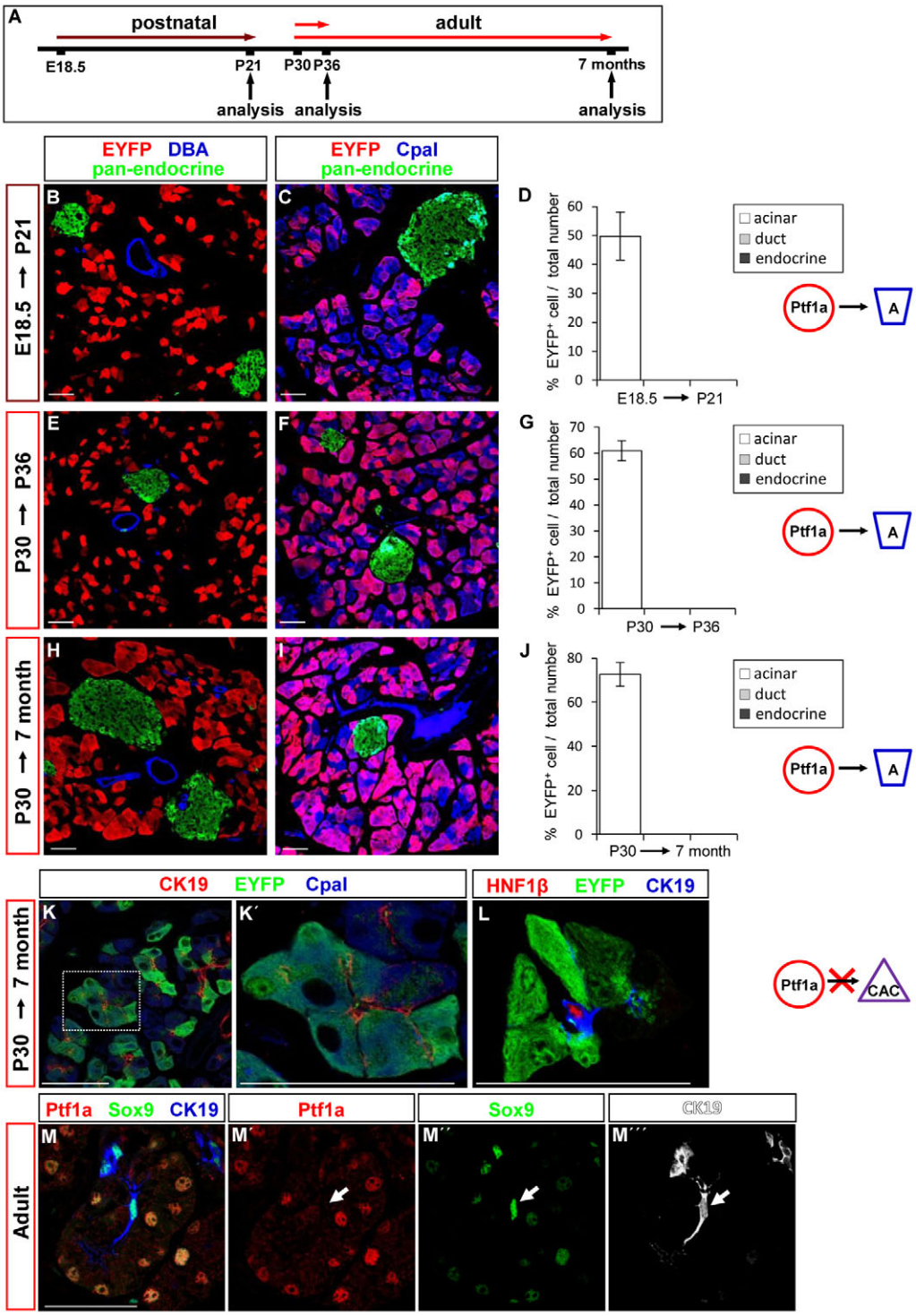

Fig. 3. *Ptf1a*-expressing cells are acinar-restricted after birth. (**A**) Postnatal/adult lineage-tracing schematic. (**B**,**C**) *Ptf1a*^{CreERTM};*R26R*^{EYFP} embryos Tam-pulsed at E18.5, analyzed 3 weeks after birth showing EYFP exclusively in acini. (**D**) P21; percentage of each pancreatic cell type expressing EYFP. (**E**,**F**,**H**,**I**) 1-month-old *Ptf1a*^{CreERTM};*R26R*^{EYFP} mice treated with Tam were chased for (E,F) 1 week or (H,I) 6 months; EYFP was only in Cpal^{+} acinar cells. (**G**,**J**) Comparing EYFP^{+} traced cells at P36 (G) or 7 months (J) showed similar acinar labeling, suggesting homeostatic acinar self-replication. (**K-L**) EYFP was absent from (K,K′) Ck19^{+} or (L) Hnf1β^{+} CAC cells after 6-month chase; diagrammed as *Ptf1a*-expressing cells not producing CACs. (**M-M′′′**) Ptf1a protein was undetectable in Sox9^{+}Ck19^{+} CACs. Scale bars: 50 μm.

multipotentiality similar to embryonic *Ptf1a*-expressing MPCs. PDL was reported to induce fairly efficient *de novo* generation of facultative Ngn3^{+} endocrine progenitors (Xu et al., 2008), and this model was chosen to evaluate whether Ptf1a^{+} acinar cells could convert toward the Ngn3^{+} population. Five-week-old *Ptf1a*^{CreERTM};*R26R*$^{EYFP/EYFP}$ mice given three doses of Tam had PDL performed 2 weeks after the last Tam injection, as described (Xu et al., 2008) (Fig. 4A). An average ~60-80% labeling efficiency was observed and strictly restricted to acinar cells (Fig. 3J); high labeling efficiency was deliberately pushed so as to detect minor populations of facultative progenitors. Pancreata were analyzed 5 days (PDL D5), 1 week (PDL D7), 4 weeks (PDL D30) or 8 weeks (PDL D60) post-PDL.

The ligated distal part of the pancreas (hereafter ‘PDL tail’), which consists of ~80% of the splenic lobe, underwent massive acinar regression by PDL D7 (supplementary material Fig. S5B,D). The unligated proximal pancreas (hereafter ‘PDL head’, comprising ~20% of the remaining unligated splenic lobe, intact gastric lobe and ventral pancreas) remained unchanged morphologically after ligation and served as a control for labeling

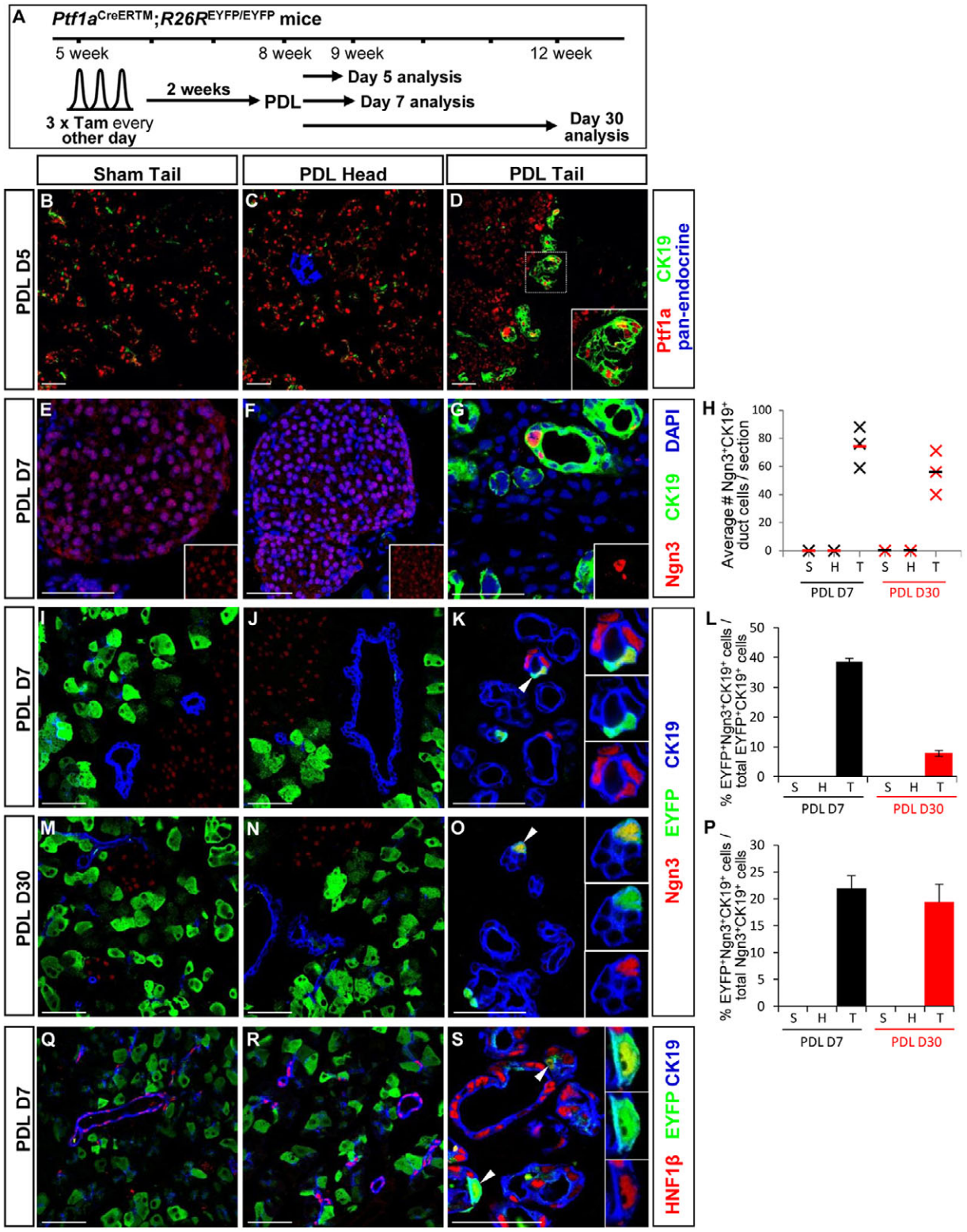

Fig. 4. PDL-induced acinar-to-ductal transdifferentiation and *de novo* Ngn3 activation. (**A**) PDL lineage-tracing schematic. (**B-F**) At D5, Ptf1a protein was found only in acini in (B) sham tail and (C) PDL head, but was in (D) PDL tail duct cells. Ngn3 was found only in islets of (E) sham tail or (F) PDL head. (**G**) *De novo* activation of Ngn3 in Ck19$^+$ duct cells, PDL tail. (**H**) Quantification, average number Ngn3$^+$Ck19$^+$ duct cells per section, PDL D7 and D30 (~10-15 sections entirely counted per PDL tail; *n*=3); solid line indicates mean. (**I**,**J**,**M**,**N**) EYFP$^+$Ngn3$^+$ cells were absent from sham tail and PDL head at (I,J) PDL D7 or (M,N) D30. (**K**,**O**) A small fraction of the Ngn3$^+$Ck19$^+$ duct cells were derived from *Ptf1a*-lineage-labeled cells (EYFP$^+$, arrowhead) in PDL tail at (K) PDL D7 and (O) D30. (**L**,**P**) Quantification of (L) percentage of EYFP$^+$Ck19$^+$ cells that were also Ngn3$^+$, and (P) percentage of EYFP$^+$Ngn3$^+$Ck19$^+$ cells over total Ngn3$^+$Ck19$^+$ cells at PDL D7 and D30. (**Q**,**R**) EYFP$^+$Ck19$^+$Hnf1β$^+$ duct cells were absent from (Q) sham tail or (R) PDL head. (**S**) *Ptf1a*-lineage-derived ducts (EYFP$^+$Ck19$^+$) were Hnf1β$^+$ (arrowhead) in PDL tail at PDL D7, indicating acinar-to-ductal transdifferentiation. Scale bars: 50 μm.

efficiency (supplementary material Fig. S5C). After PDL, the total pancreatic epithelial area of PDL tail was dramatically reduced, while overall pancreatic weight remained similar because acini were replaced by fibrotic and inflammatory cells; islets and duct cells were spared and the animals remained euglycemic (supplementary material Fig. S5C-H) (Xu et al., 2008). Post-PDL D5, tubular complexes composed of Ck19$^+$ ducts started to form in the PDL tail. Ptf1a protein was detected in these tubular complexes at this stage but not in the ducts of the PDL head, or the control sham-operated tail (hereafter 'sham tail'; Fig. 4B-D; supplementary material Fig. S5A). The presence of Ptf1a protein in ductal cells proximate to the regressing acini might reflect detection of the early stages of acinar-to-ductal conversion. An alternate explanation is that remodeling ducts activated *Ptf1a* expression; a hypothesis ruled out by two observations: (1) the lack of Ptf1a protein by immunolabeling in the Ck19$^+$/Hnf1β$^+$ tubular complexes at PDL D7, D30 and D60 (supplementary material Fig. S6B-M); and (2) Tam treatment of *Ptf1a*^{CreERTM};R26R$^{EYFP/EYFP}$ mice post-PDL D7, after acini involution was almost completed, such that CreER would only label duct cells activating *Ptf1a* expression. By this strategy, extremely rare *Ptf1a*-lineage-labeled duct cells (~1-2 EYFP$^+$Ck19$^+$ every three sections, possibly derived from late incorporation into the tubular complexes of the 1% acinar cells that escape involution) were found at post-PDL D30 and D60 (supplementary material Fig. S7E-K). Taken together, these results indicate that duct cells did not activate *Ptf1a* expression.

One week post-PDL, ~99% of acinar cells in the PDL tail had involuted, and the remodeled ducts formed highly proliferative tubular complexes. The PDL tail was fibrotic and infiltrated with inflammatory cells (supplementary material Fig. S5A-D). As previously reported (Xu et al., 2008), we detected Ngn3 protein in Ck19$^+$ duct cells in the PDL tail at post-PDL D7 (Fig. 4G; supplementary material Fig. S8A-A″) and D30 (Fig. 4M-O; Fig. S8B-B″). A low Ngn3 signal was detected in islet cells, as reported (Wang et al., 2009), but not in the ducts of the sham tail or PDL head tissues (Fig. 4E,F). An average of 74 (PDL D7) and 56 (PDL D30) Ngn3$^+$Ck19$^+$ duct cells were found per section (~10-15 sections counted per PDL tail pancreas) (n=3; Fig. 4H). Scattered rare Ngn3$^+$Ck19$^+$ duct cells were also found at post-PDL D60 (not shown), consistent with the previous post-PDL analysis showing *Ngn3* mRNA expression peaking at post-PDL D7 and reducing by later time points (Xu et al., 2008). These data also imply that the majority of the early Ngn3$^+$Ck19$^+$ protoendocrine cells have moved on to another differentiation state at later time points post-PDL. Notably, the Ngn3 signal was much higher in duct cells than in the islet endocrine cells (Fig. 4F,G, inset). These data imply that while Ngn3 is required for proper function/maintenance of adult endocrine cells (Wang et al., 2009), Ngn3$^+$ duct cells arose from *de novo* activation of endocrine progenitor behavior upon injury, resembling the embryonic endocrine neogenesis process.

To determine whether acinar cells contribute to regeneration of the duct and endocrine pancreas after PDL, we used *Ptf1a*^{CreERTM} to lineage-trace the Ptf1a$^+$ acinar cells and their progeny. In PDL tail post-PDL D7, we observed small numbers of EYFP$^+$ cells in Ck19$^+$ ducts, suggesting that some of the *Ptf1a*-lineage-labeled acinar cells escaped involution but became integrated into the tubular complex (Fig. 4Q-S; supplementary material Fig. S7A-D; Fig. S8F-H). The number of EYFP$^+$Ck19$^+$ duct cells increased substantially from post-PDL D7 to D60 (from 5.8±1.1% to 25.4±5.14% of total Ck19$^+$ duct, respectively; n=3; supplementary material Fig. S7A-D,A′-C′), consistent with a continued high proliferative capacity as detected by BrdU incorporation (supplementary material Fig. S5E-G,I). EYFP$^+$Ck19$^+$ duct cells were also found to produce Hnf1β (Fig. 4Q-S; supplementary material Fig. S8C-E) and Sox9 (supplementary material Fig. S8F-K) or both (supplementary material Fig. S8L-N), at post-PDL D7 and D30. Detection of Hnf1β and Sox9 protein in these EYFP$^+$ ducts at post-PDL D7 suggests that, after PDL, the Ptf1a$^+$ acinar cells de-differentiated to a more primitive epithelium resembling the embryonic trunk epithelium of the 2° transition. Furthermore, we did not observe any amylase$^+$Hnf1β$^+$ transitional cell state at PDL D7 (supplementary material Fig. S9A,B), suggesting that acinar enzymes were downregulated before the activation of multipotency factors.

The presence of EYFP$^+$Ngn3$^+$Ck19$^+$ duct cells in the tail region post-PDL D7 (Fig. 4I-K) and D30 (Fig. 4M-O) suggested their derivation from *Ptf1a*$^+$-acinar-derived duct cells. Of total Ngn3$^+$Ck19$^+$ duct population, 21.9±2.4% (PDL D7) and 19.4±3.3% (PDL D30) were EYFP$^+$Ngn3$^+$Ck19$^+$ (Fig. 4P). Notably, not all EYFP$^+$ duct cells were Ngn3$^+$, indicating either: (1) incomplete *R26R*^{Eyfp} lineage labeling; or (2) not all Ngn3$^+$ duct cells originated from *Ptf1a*-lineage cells (possibly originating from the duct proper); and/or (3) while some *Ptf1a*$^+$-acinar-derived new duct cells went on to activate *Ngn3* expression as they commit toward the endocrine lineage, others remain stably integrated as mature duct epithelial cells. The EYFP$^+$Ngn3$^+$Ck19$^+$ cells comprised 38% of the total EYFP$^+$Ck19$^+$ cell number at post-PDL D7 and became reduced to 8% at post-PDL D30 (n=3; Fig. 4L). It is possible that there was a higher proliferative capacity of *Ptf1a*-lineage-derived (EYFP$^+$Ck19$^+$) duct cells, compared with protoendocrine EYFP$^+$Ngn3$^+$Ck19$^+$ cells. Taken together, these data suggest that after PDL, significant numbers of Ptf1a$^+$ acinar cells trans-differentiated into ductal cells with a portion of these duct cells being competent to activate expression of the endocrine commitment factor Ngn3.

Long-term reprogramming of Ptf1a$^+$ acinar to endocrine cells after PDL

To assess whether Ptf1a$^+$ cells can give rise to endocrine cells after injury, particularly focusing on β-cells, pancreata from *Ptf1a*^{CreERTM};*R26R*$^{EYFP/EYFP}$ mice lineage-labeled by Tam treatment prior to PDL were analyzed, first at post-PDL D30 (Fig. 5A). In order to increase the sensitivity of detecting a potentially small population of endocrine cells derived from Ptf1a$^+$ facultative progenitors, we performed an extensive, systematic analysis across a large portion of each pancreas. Thus, we analyzed ~40-45 sections from each mouse (~10% of total sections from each tail or head region) spaced evenly across the entire PDL tail, sham tail and PDL head region, and visually scanned the entire section for EYFP$^+$endocrine-hormone$^+$ cells (with an insulin, glucagon, somatostatin and pancreatic-polypeptide antibody cocktail) or EYFP$^+$insulin$^+$ cells (see supplementary material Fig. S10 for quantitation strategy). No EYFP$^+$ endocrine cells were observed in the sham tail or PDL head after PDL (Fig. 5B,C,N,O), solidifying the absence of leakiness of *Ptf1a*^{CreERTM} allele and consistent with the adult lineage-tracing above (Fig. 3J). We did not detect any EYFP$^+$endocrine-hormone$^+$ cells or EYFP$^+$insulin$^+$ cells either in islets or ducts proper in post-PDL D30 tail (n=4; Fig. 5D,E).

To investigate rigorously whether new endocrine/β-cells could be generated from Ptf1a$^+$ cells in a more chronic timeframe post-PDL, we analyzed Tam-treated *Ptf1a*^{CreERTM};*R26R*$^{EYFP/EYFP}$ pancreata 8 weeks post-PDL (D60), a period substantially longer than most previous PDL studies. More Ck19$^+$ duct clusters than at post-PDL D60 were EYFP$^+$. Many foci of tubular-complexes, individually almost completely labeled (Fig. 5L), were distributed

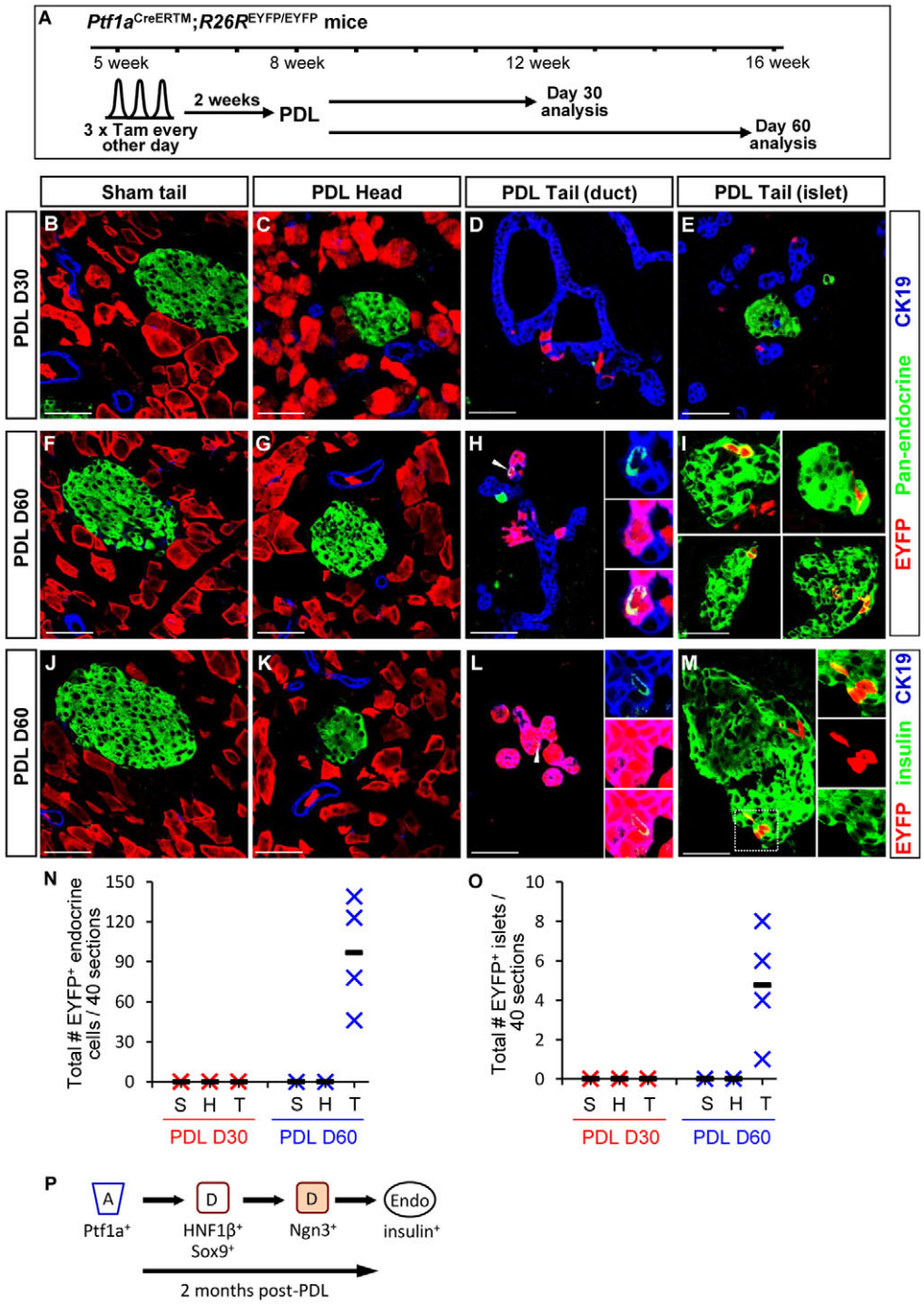

Fig. 5. Ptf1a$^+$ acini transdifferentiate into endocrine cells, likely via Ck19$^+$ ductal intermediates, 2 months post-PDL. (**A**) Lineage-tracing schematic. (**B-M**) EYFP$^+$ cells were absent from duct and endocrine compartment in (B) sham tail, and (C) PDL head, at post-PDL D30. *Ptf1a*-lineage-labeled cells (EYFP$^+$) were detected in (D) Ck19$^+$ ducts, but not (E) endocrine cells in PDL tail at PDL D30. At post-PDL D60, while EYFP$^+$ cells were found only in acini in (F,J) sham tail or (G,K) PDL head, EYFP$^+$hormone$^+$ cells were detected (H) in or closely apposed to Ck19$^+$ ducts, and (I) in islets in PDL tail. Some of these cells are insulin$^+$ in (L) ducts and (M) islets. (**N**,**O**) Total number of (N) EYFP$^+$ endocrine cells and (O) EYFP$^+$ islets (40 sections, ~10% of PDL tail or head; *n*=4) at PDL D30 and D60; solid line indicates mean. (**P**) Summary of PDL lineage-tracing results. S, sham tail; H,T: PDL head, tail. Scale bars: 50 µm.

throughout the tissue and accounted for 25.4±5.14% of the total Ck19$^+$ duct area. This representation was 11.6±1.81% at post-PDL D30, suggesting that proliferation and expansion of the *Ptf1a*-lineage-labeled duct/tubular-complex cells continued from D30 to D60 (*n*=3; supplementary material Fig. S7B-D). We also detected in post-PDL D60 tissue a small but significant number of EYFP$^+$endocrine-hormone$^+$ cells in Ck19$^+$ ducts (Fig. 5H), as well as in islets (Fig. 5I). Around 75% of the EYFP$^+$hormone$^+$ cells were located in/at the ducts, whereas ~25% were found in the islets. Some of these endocrine cells, either in the ducts or in islets, were also insulin-producing (Fig. 5L,M), suggesting that β-cells can be derived from Ptf1a$^+$ acinar cells after PDL. Most importantly, these Ptf1a-lineage-derived insulin$^+$ cells produced several mature β-cell transcription factors, such as Pdx1^{HI} (Fig. 7A,B), Nkx6.1 (Fig. 7E,F), and MafA (Fig. 7I,J), indicating a mature β-cell status. Most of the EYFP$^+$insulin$^+$ cells were presents as singlet β-cells located at/in the ducts and did not produce GLUT2 (data not shown). The lack of β-β cell contact may prevent membrane localization of GLUT2 in these EYFP$^+$ singlet β-cells as previously suggested (Orci et al., 1989; Gannon et al., 2000). Extensive, systematic quantification revealed 965±393 EYFP$^+$hormone$^+$ endocrine cells, per PDL tail analyzed (*n*=4; Fig. 5N). We only observed one to eight islets per 10% of PDL tail containing EYFP$^+$ endocrine cells; in such islets only ~5-10% of the cells were EYFP$^+$ (*n*=4; Fig. 5O; data not shown). Because ~99% of acinar cells were lost at post-PDL D7, and the persistent

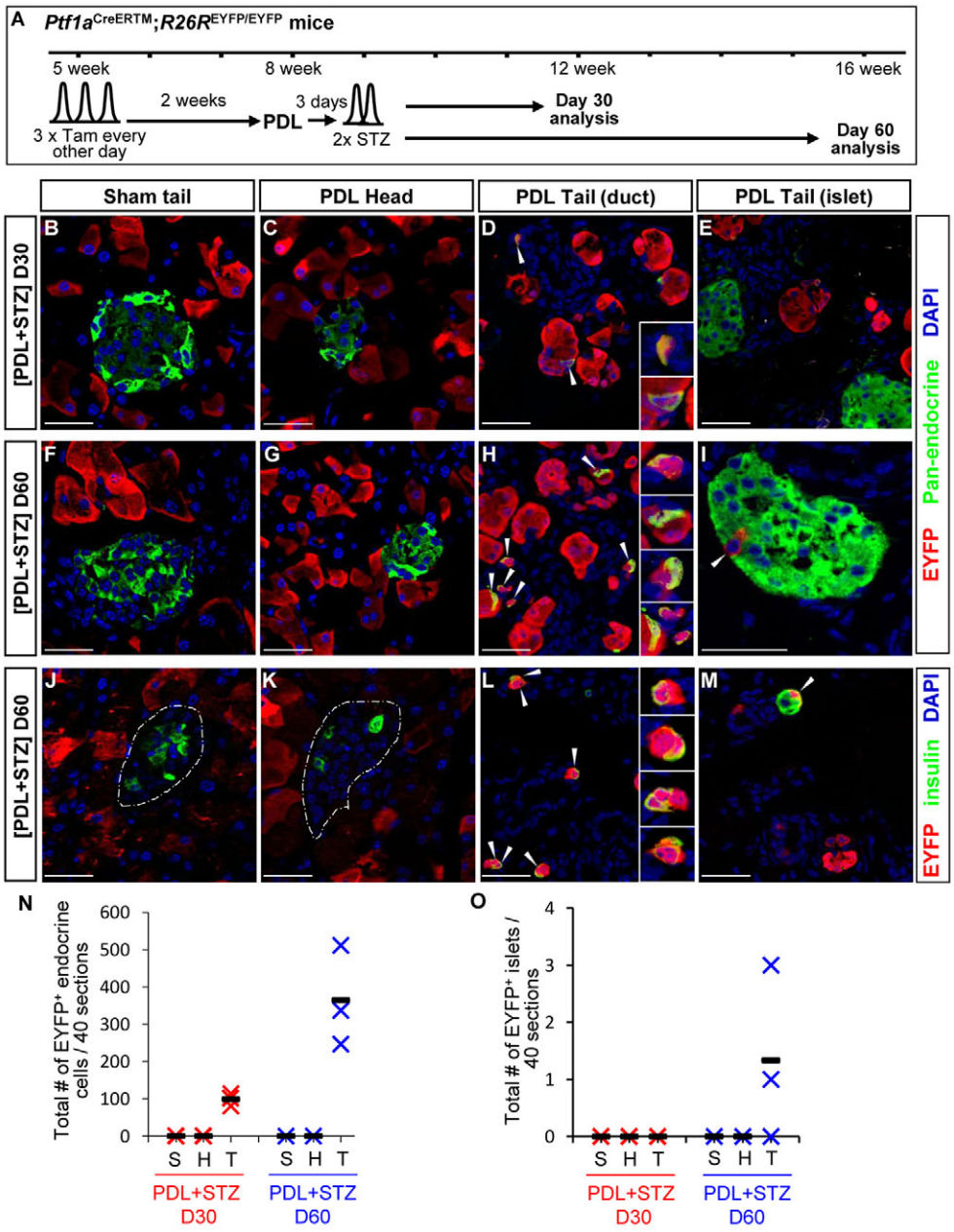

Fig. 6. [PDL+STZ] enhances acinar-to-endocrine transdifferentiation. (**A**) [PDL+STZ] lineage-tracing schematic. (**B-M**) At [PDL+STZ] D30, no EYFP$^+$ cells were present in duct or endocrine compartment in either (B) sham tail or (C) PDL head. EYFP$^+$hormone$^+$ cells were detected 30 days post-[PDL+STZ] in (D) the vicinity of ducts but (E) not in islets. At post-[PDL+STZ] D60, EYFP$^+$ cells were only in acini in (F,J) sham tail and (G,K) PDL head, but numerous EYFP$^+$endocrine-hormone$^+$ cells in PDL tail were (H) apposed to ducts or (I) in islets. Of these, EYFP$^+$insulin$^+$ cells were found (L) near/in ducts or (M) in small islet clusters. (**N**,**O**) Quantitation of (N) total number EYFP$^+$ endocrine cells and (O) total number EYFP$^+$ islets (40 sections, ~10% of PDL tail or head; *n*=3) at post-[PDL+STZ] D30 and D60; solid line indicates mean. S, sham tail; H, T: PDL head, tail. Scale bars: 50 μm.

blockage of the pancreatic duct limits acinar regeneration, we believe that these EYFP$^+$ endocrine cells were originated from Ptf1a$^+$ acinar-derived duct cells, rather than arising directly from Ptf1a$^+$ acini as no amylase$^+$insulin$^+$ transitional intermediate was found at PDL D7, D30 and D60 (supplementary material Fig. S9C-H). We did not detect any EYFP$^+$ cells in the endocrine compartment for either sham tail or PDL head at post-PDL D60 (Fig. 5F,G,J,K,N,O). These *in vivo* lineage-tracing data support the proposal that Ptf1a$^+$ acinar cells could be stimulated to become facultative progenitors and undergo a long-term (albeit inefficient) reprogramming to endocrine cells, via a ductal intermediate, in the PDL-injury/regeneration context (Fig. 5P).

Enhanced acinar-to-duct-to-endocrine conversion with pre-existing β-cell ablation

Because islet cells were spared and mice remained euglycemic after PDL, we propose that the lack of hypothetical physiological stimuli to produce additional β-cells could explain the low level conversion to endocrine cells from Ptf1a$^+$ acini-derived duct cells. We reasoned that eliminating some pre-existing β-cells could provide one such physiological cue (perhaps including the ensuing hyperglycemia), and addressed the deep injury context of PDL plus β-cell destruction. Tam-treated *Ptf1a*^{CreERTM};*R26R*$^{EYFP/EYFP}$ mice were given two consecutive doses of STZ three days post-PDL to kill a portion of β-cells, and pancreata were analyzed 30 and 60 days post-PDL (Fig. 6A). We observed ~50-70% reduction in β-cell numbers with this protocol, and mice became hyperglycemic (ad lib feeding blood glucose level >450 mg/dl) 2-3 days after STZ treatment (supplementary material Fig. S10B).

To determine if [PDL+STZ] treatment could speed up acinar-to-endocrine conversion, we analyzed pancreata post-PDL D30. [PDL+STZ]-treated mice remained hyperglycemic at this time (supplementary material Fig. S10B). We did not treat mice with any β-cell-proliferation-stimulating agents (e.g. insulin, GLP or

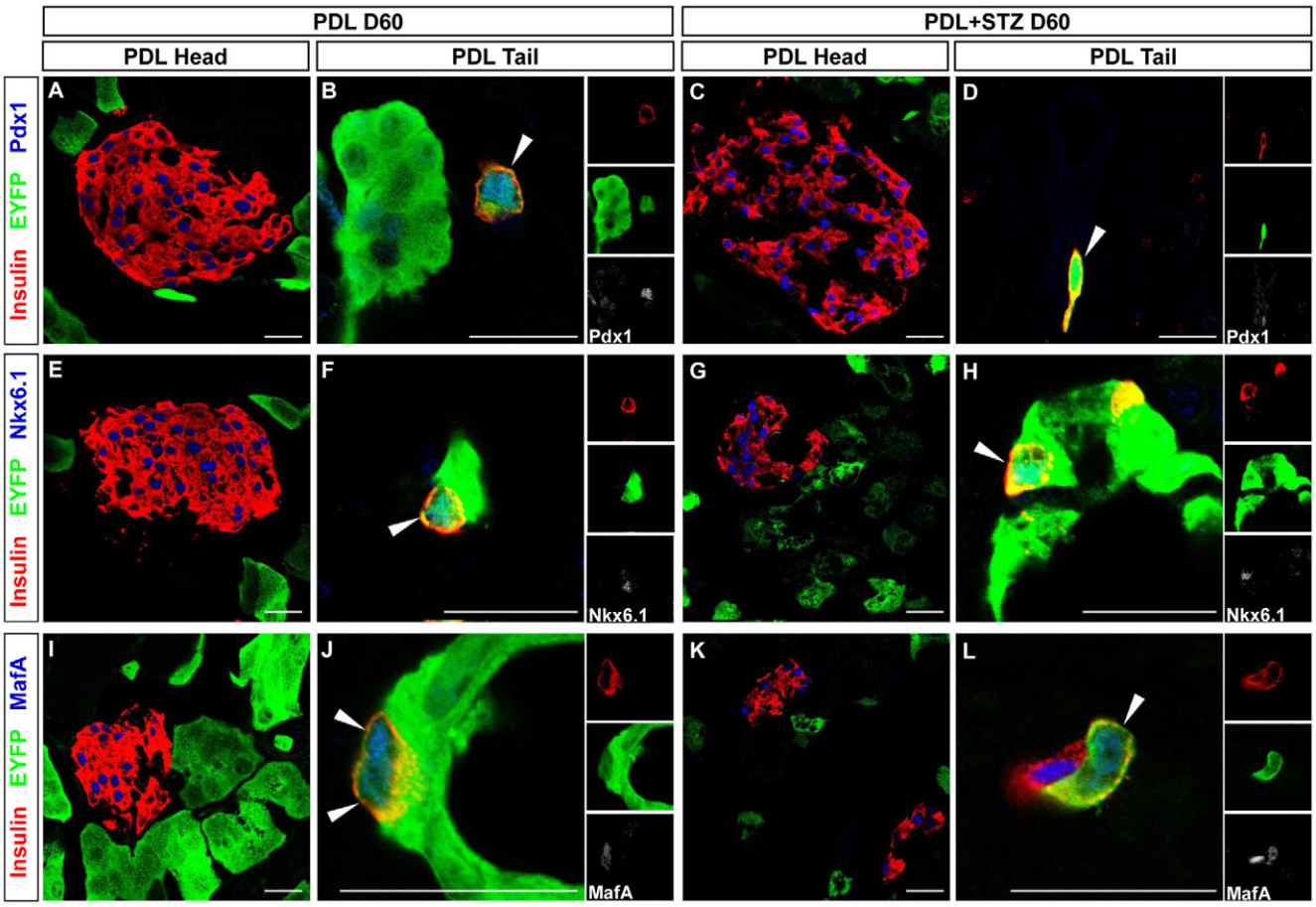

Fig. 7. *Ptf1a*-lineage-labeled insulin$^+$ cells produced mature β-cell transcription factors. Mature islet β-cells in PDL head tissue produced (**A**,**C**) Pdx1^{HI}, (**E**,**G**) Nkx6.1, (**I**,**K**) MafA. EYFP$^+$insulin$^+$ cells from tail tissues of PDL D60 and [PDL+STZ] D60 were similarly (**B**,**D**) Pdx1^{HI}, (**F**,**H**) Nkx6.1$^+$ and (**J**,**L**) Mafa$^+$. Scale bars: 20 μm.

EGF/gastrin), under the logic that avoiding such agents might promote transdifferentiation and disfavor replication of β-cells. We found EYFP$^+$endocrine-hormone$^+$ cells mostly located either in ducts, or duct-apposed, in [PDL+STZ] tail tissue already by post-PDL D30, notably different from PDL alone at D30 (Fig. 6D; for more examples see supplementary material Fig. S11A). No EYFP$^+$endocrine-hormone$^+$ cells were found in the PDL head or STZ-treated sham tail (Fig. 6B,C), suggesting strongly that STZ alone did not induce acinar-to-endocrine transdifferentiation. The numbers of EYFP$^+$endocrine-hormone$^+$ cells found in [PDL+STZ] D30 tail tissue were similar to those found post-PDL D60 tail without STZ treatment (average 990±149 EYFP$^+$endocrine-hormone$^+$ cells per PDL tail in [PDL+STZ] D30, compared to 965±393 EYFP$^+$ endocrine-hormone$^+$ cells per PDL tail at PDL D60; *n*=3 separate animals; compare Fig. 6N with Fig. 5N). At post-[PDL+STZ] D60, the numbers of EYFP$^+$endocrine-hormone$^+$ cells had increased ~3-4.5 fold over D30 (average 3653±1205 EYFP$^+$endocrine-hormone$^+$ cells per PDL tail tissue; *n*=3; Fig. 6N). EYFP$^+$insulin$^+$ cells were also found at post-[PDL+STZ] D30 and D60 (Fig. 6L,M; see more examples in supplementary material Fig. S11A,B). These EYFP$^+$insulin$^+$ cells were also Pdx1HI (Fig. 7C,D), Nkx6.1$^+$ (Fig. 7G,H), and Mafa$^+$ (Fig. 7K,L), suggesting that they are mature β-cells. Notably, fewer EYFP$^+$endocrine-hormone$^+$ cells were located within islets under the [PDL+STZ] condition compared to PDL alone at day 60 (average ~1 islet per 10% PDL tail labeled in post-[PDL+STZ] D60, versus average ~5 islets per 10% PDL tail in post-PDL D60; compare Fig. 5O; Fig. 6O). We hypothesize that repellents or toxics released from apoptotic β-cells after STZ treatment might render the islets unattractive to home Ptf1a-lineage-derived endocrine cells. Taken together, these findings demonstrated that the deep lesion enhanced acinar-to-endocrine transdifferentiation rate and efficiency compared to PDL alone.

DISCUSSION

We are still far from understanding how dynamic cell heterogeneity and intercommunication connect to epithelial morphogenesis and cell-fate allocation, and if certain mature cells retain homeostatic or facultative multipotency/plasticity. Our immuno-colocalization of TFs considered as progenitor-defining revealed heterogeneity as epithelial morphogenesis begins at E11.5-12.5, well before the 2° transition stage. The putative Ptf1a$^+$Sox9$^+$Hnf1β$^+$ MPCs (the same signature as early MPCs), possibly under the influence of localized signals from the mesenchyme, become localized to the tip epithelium and progressively diminish between E12.5 and E15.5. The reduction in these putative MPCs parallels the quantitative decrease in progeny of *Ptf1a*-expressing cells that enter non-acinar lineages. After the 2° transition (E15.5 onward), Ptf1a$^+$ MPC activity becomes very low, and *Ptf1a*-expressing cells are acinar-unipotent by late gestation and in adults.

More importantly, we showed that PDL or [PDL+STZ] induced restoration of an early-organogenesis-like MPC competence in adult acinar cells, with probably stepwise redifferentiation into ducts then endocrine cells. Ptf1a^{+} acinar cells reactivated embryonic multipotency markers, differentiating rapidly into long-lived duct cells. Some *Ptf1a*-derived duct cells activated Ngn3, and some *Ptf1a*-lineage-derived cells progressed to endocrine cells, including Pdx1^{HI}/Nkx6.1^{+}/MafA^{+}/insulin^{+} β-cells. This conversion occurred without exogenous factors such as β-cell-instructive TFs or intercellular signaling factors.

Progressive lineage restriction of Ptf1a-expressing cells

We have more carefully enumerated the multi-to-unipotential switch during organogenesis, with findings largely consistent but with novel aspects compared to the previous *CpaI*^{CreER} study (Zhou et al., 2007), but it is also important that we used an MPC-instructive gene *Ptf1a*, and not a *Ptf1a* surrogate encoding a digestive enzyme, which should have no regulatory role in MPC formation/maintenance. Furthermore, our E10.5 immuno-colocalization data (supplementary material Fig. S12) showed CpaI in ~65% of Ptf1a^{+} cells (all CpaI^{+} cells were Ptf1a^{+}), suggesting CpaI only partially marks MPC. Our *Ptf1a*^{CreERTM}-based analysis validates the *CpaI*^{CreER} study but elaborates a stronger understanding of the dynamic nature of MPC location during tip-trunk segregation in the 2° transition.

The *CpaI*^{CreER} study proposed that CpaI^{+} tip MPC contribute significantly to the expansion of the trunk epithelium (endocrine/duct bipotent progenitor compartment) after E12, but we found that *Ptf1a*-expressing cells seeded the trunk epithelium until E13.5, with only a small contribution at/after ~E12.5. We can conclude that tip seeds trunk is a minor influence during the true 2° transition, consistent with the proposal that intra-trunk proliferation and plexus remodeling (Villasenor et al., 2010) cause most of the growth and extension of the trunk epithelium.

We note that the Ptf1a^{+}Pdx1^{+}CpaI^{+}cMyc^{HI} MPC proposed in Zhou et al. (Zhou et al., 2007) did not refer to tip heterogeneity, and in fact differentiated acini retain that signature. Solar et al. (Solar et al., 2009) suggested that Hnf1β^{+} trunk cells are multipotent between E11.5-13.5, but did not rule out that *Hnf1β*^{CreER}-traced MPC could be an Hnf1β^{+}CpaI^{+} tip subset. Furthermore, considering the tip-trunk interface Nkx6.1^{+}Ptf1a^{+}Sox9^{+}Pdx1^{+} MPC proposed by Kopp et al. (Kopp et al., 2011), which lacked Hnf1β, the Ptf1a^{+}Sox9^{+} putative tip MPC we detected were Hnf1β^{+}, and distributed heterogeneously, both intra-tip and at the tip-trunk interface. The Ptf1a^{+}Sox9^{+}Hnf1β^{+} tip MPC could be the same as those detected by Solar et al. (Solar et al., 2009) and Kopp et al. (Kopp et al., 2011), leading to the generalization that multipotentiality is preserved in the tip, not trunk, domain. What controls tip-trunk compartmentalization, and which signals are present in the local tip microenvironment that determine this MPC niche, represent interesting aspects for future studies.

Postnatal lineage restriction of Ptf1a^{+} cells

Postnatal Ptf1a^{+} cells only produced acinar cells, agreeing with the results of *Elastase*^{CreERT2} studies showing homeostatic maintenance of this compartment comes from acinar replication (Desai et al., 2007). A *Sox9*^{CreER} knock-in study (Furuyama et al., 2011) seems contradictory, in suggesting that ~80% of acinar cells came from Sox9^{+} duct or centroacinar cells following a one-year post-Tam chase. We found no significant reduction in the proportion of *Ptf1a*^{CreERTM}-labeled acini after a 6-month chase, arguing against dilution from other cell populations. This discrepancy could be reconciled, bearing in mind the lower level *Sox9* expression in adult acini (Kopp et al., 2011; Dubois et al., 2011) (Fig. 3M,M″), such that the high tamoxifen dosage used (5×4 mg) in Furuyama et al. (Furuyama et al., 2011), would broadly and directly activating the reporter allele in acini.

Facultative PDL-induced MPC behavior in adult acinar cells

The mass of acinar cells and their relatively close developmental history with endocrine cells lead to ideas that partial reprogramming *in vivo* might offset a β-cell deficit without compromising organ function (Pan and Wright, 2011). Zhou et al. (Zhou et al., 2008) reported reprogramming of acini to β-like fate using a viral cocktail of β-cell TFs: Pdx1, Ngn3 and MafA. Our evidence suggests that Ptf1a^{+} acinar cells possess facultative progenitor potential under PDL, allowing them quickly to produce long-lived ducts and later-arising endocrine/β-cells. Several *in vitro* studies suggested acinar-to-β-cell conversion with EGF, nicotinamide, TGFα or combination(s) treatment (Baeyens et al., 2005; Minami et al., 2005). Non-autonomous effects of tissue dissociation might substantially affect *in vitro* conversion. Genetic lineage-tracing was not included in the previous reports of *in vivo* acinar-to-endocrine transdifferentiation (purportedly involving amylase^{+}insulin^{+} intermediates) in 24-hour post-PDL rats (Bertelli and Bendayan, 1997). Our study therefore provides rigorous *in vivo* evidence for PDL-induced acinar-to-endocrine conversion. We contradict the conclusion from *Elastase*^{CreERT2} lineage-tracing *in vivo* that acini did not seed duct or endocrine fates after Ppx, PDL and cerulean-induced pancreatitis (Desai et al., 2007), but the 30% acinar labeling efficiency (compared to our ~80% labeling, assessing large amounts of the organ and over a long period) might have failed to detect low-level contributions.

If there is any cryptic destabilization of the acinar program from *Ptf1a* heterozygosity (*Ptf1a*^{CreERTM} is a null allele), there are consequences only under injury, and *Ptf1a*$^{CreER/+}$ mice have normal embryonic and adult pancreas. Distinct Ptf1a levels might control the interaction with the RBP-J or RBP-JL partner in the PTF1 complex. Ptf1a associates with RBPJ (PTF1^{RBPJ}) in MPC, but with *RBPJL* (PTF1^{RBPJL}) in proacinar/acinar cells (Masui et al., 2007), with the PTF1^{RBPJ}-to-PTF1^{RBPJL} switch likely essential for facilitating epithelial tip-trunk compartmentalization (Masui et al., 2007; Schaffer et al., 2010). Under injury, reduced Ptf1a levels could allow reformation of PTF1^{RBPJ}, which together with Sox9/Hnf1β production leads to reacquisition of MPC character. Future studies will be directed toward understanding how differential Ptf1a levels affect multipotency restoration in Ptf1a^{+} acini during injury.

Acinar-to-endocrine conversion could be aided by disturbances in the extracellular environment, including the chronic inflammation-associated signals in PDL. Cytokines may also influence pancreas regeneration (Homo-Delarche and Drexhage, 2004), and invading macrophages may suppress islet loss during exocrine degeneration (Tessem et al., 2008). Wang et al. (Wang et al., 2007) suggested a role for immune-reaction effects against adenovirus in liver-to-β-like cell conversions driven by pro-endocrine TFs (Pdx1, Ngn3). Our *Ptf1a*-lineage-labeled endocrine cells were often found next to duct-apposed small endocrine clusters. Such clusters are distributed throughout PDL pancreas, although some might arise from duct cells proper (Xu et al., 2008). Speculatively, acinar-derived endocrine cells could home to these small endocrine clusters rather than to islets proper, or endocrine

cell migration from their birthplace in the tubular complexes might be hindered by the altered fibrotic stroma.

While we showed that Ptf1a$^+$ acinar cells produced Ck19$^+$Hnf1β$^+$Sox9$^+$ primitive ductal intermediates, Ngn3$^+$ endocrine progenitors and hormone$^+$ endocrine cells, showing directly a sequential movement through these transitional states would need either real-time tracing, or dual/multiplex genetic lineage-tracing methods (e.g. combining Cre/LoxP, Dre/Rox or FLPe/FRT). We did not observe any pan-endocrine/insulin co-label with acinar markers arguing against a direct rapid conversion from acini to endocrine cells.

Reproliferative CACs have been suggested as facultative progenitors under injury. Rovira et al. (Rovira et al., 2010) detected *Ptf1a* by RT-PCR in Aldh1$^+$ CACs, and MPC competence in CAC-derived pancreatospheres. We failed to detect Ptf1a protein in CACs, and adult lineage-tracing with *Ptf1a*^{CreERTM} did not label CACs. It was still possible that *Ptf1a* expression could be activated in CACs post-PDL, which incorporated into tubular complexes and yielded duct/endocrine cells. However, Tam-induction at post-PDL D7 (when acinar involution is essentially complete) only labeled extremely scarce, if any, duct cells, and no endocrine cells, at post-PDL D30 and D60, strongly arguing against any relevant post-PDL acquisition of *Ptf1a* expression by CAC or duct. Lineage-tracing using lines that label CACs (*Hnf1β*^{CreERT2}, *Sox9*^{CreERT2}, *Hes1*^{CreERT2}) showed no evidence for endocrine cell production post-PDL (Solar et al., 2009; Kopp et al., 2011; Kopinke et al., 2011). The simplest conclusion is that our labeled endocrine cells originated from sequential acinar-to-duct-to-endocrine transdifferentiation.

Deep lesion [PDL+STZ] enhances acinar-to-endocrine conversion

β-Cell destruction by STZ enhanced PDL-induced transdifferentiation. We reasoned that the relative scarcity under PDL alone reflected the absence of a 'call for more β-cells'. One candidate signal under [PDL+STZ] is glucose, a stimulant of β-cell replication after ablation (Porat et al., 2011). Under [PDL+STZ] condition, we observed no significant restoration of β-cell mass after 60 days nor improved glycemia (few β-cells being derived from *Ptf1a*$^+$ cells). Future study could determine the signals (hyperglycemia and inflammatory signals from the attacked islets) that contribute to the increased stimulus for acinar to endocrine transformation under [PDL+STZ]. And, if reinduction of MPC character in the adult under injury recapitulates any of the steps of earlier embryonic endocrine ontogeny.

[PDL+STZ]-induced endocrine cell interconversion has been reported. Chung et al. (Chung et al., 2010) proposed an α/β intermediate as a precursor for β-cells post-injury, although there was no lineage-tracing analysis. Another non-PDL study (Thorel et al., 2010) used lineage tracing to show α-to-βconversion after near-total β-cell elimination. In our study, only a subset of cells derived from *Ptf1a*-expressing facultative progenitors were mature β-cells, and we are unable to comment on interconversion between hormone cell types.

Our evidence that adult pancreatic acini are facultatively plastic provides impetus for determining how injury epigenetically destabilizes the acinar program, influence of niche perturbation and signals from inflammatory cells, and if only certain acinar cells are conversion-competent. The low rate of endocrine conversion could be analogous to generating induced pluripotent stem cells (iPSCs), where a tiny fraction of the initial differentiated population is captured via their induced growth potential; indeed, endocrine conversion might increase under strategies similar to those applied to iPSCs. Our findings might lead to pharmacological intervention using small molecules that modulate the epigenetic landscape or mimic inflammatory signaling. Controlling plasticity might allow regulated reprogramming as an alternative to cell transplantation.

Acknowledgements
We thank Jill Lindner and Susan Hipkens for performing RMCE; Maike Sander, Ben Stanger, Jane Johnson for Ngn3, Ck19 and Ptf1a antibodies, and Guoqiang Gu and Wright Lab members for discussions. Immunofluorescent images were gathered in part using the VUMC Cell Imaging Shared Resource (supported by NIH grants CA68485, DK20593, DK58404 and DK59637).

Funding
Support was from the Juvenile Diabetes Research Foundation (JDRF) to F.C.P. and National Institutes of Health [U19 DK 042502 and U01 DK 089570] to C.V.E.W. Deposited in PMC for release after 12 months.

Competing interests statement
The authors declare no competing financial interests.

Supplementary material
Supplementary material available online at
http://dev.biologists.org/lookup/suppl/doi:10.1242/dev.090159/-/DC1

References

Ahn, S. and Joyner, A. L. (2004). Dynamic changes in the response of cells to positive hedgehog signaling during mouse limb patterning. *Cell* **118**, 505-516.
Baeyens, L., De Breuck, S., Lardon, J., Mfopou, J. K., Rooman, I. and Bouwens, L. (2005). In vitro generation of insulin-producing beta cells from adult exocrine pancreatic cells. *Diabetologia* **48**, 49-57.
Bertelli, E. and Bendayan, M. (1997). Intermediate endocrine-acinar pancreatic cells in duct ligation conditions. *Am. J. Physiol.* **273**, C1641-C1649.
Bouwens, L. and Rooman, I. (2005). Regulation of pancreatic beta-cell mass. *Physiol. Rev.* **85**, 1255-1270.
Burlison, J. S., Long, Q., Fujitani, Y., Wright, C. V. and Magnuson, M. A. (2008). Pdx-1 and Ptf1a concurrently determine fate specification of pancreatic multipotent progenitor cells. *Dev. Biol.* **316**, 74-86.
Chung, C. H., Hao, E., Piran, R., Keinan, E. and Levine, F. (2010). Pancreatic β-cell neogenesis by direct conversion from mature α-cells. *Stem Cells* **28**, 1630-1638.
Danielian, P. S., Muccino, D., Rowitch, D. H., Michael, S. K. and McMahon, A. P. (1998). Modification of gene activity in mouse embryos in utero by a tamoxifen-inducible form of Cre recombinase. *Curr. Biol.* **8**, 1323-1326.
Desai, B. M., Oliver-Krasinski, J., De Leon, D. D., Farzad, C., Hong, N., Leach, S. D. and Stoffers, D. A. (2007). Preexisting pancreatic acinar cells contribute to acinar cell, but not islet beta cell, regeneration. *J. Clin. Invest.* **117**, 971-977.
Dubois, C. L., Shih, H. P., Seymour, P. A., Patel, N. A., Behrmann, J. M., Ngo, V. and Sander, M. (2011). Sox9-haploinsufficiency causes glucose intolerance in mice. *PLoS ONE* **6**, e23131.
Furuyama, K., Kawaguchi, Y., Akiyama, H., Horiguchi, M., Kodama, S., Kuhara, T., Hosokawa, S., Elbahrawy, A., Soeda, T., Koizumi, M. et al. (2011). Continuous cell supply from a Sox9-expressing progenitor zone in adult liver, exocrine pancreas and intestine. *Nat. Genet.* **43**, 34-41.
Gannon, M., Ray, M. K., Van Zee, K., Rausa, F., Costa, R. H. and Wright, C. V. (2000). Persistent expression of HNF6 in islet endocrine cells causes disrupted islet architecture and loss of beta cell function. *Development* **127**, 2883-2895.
Granger, A. and Kushner, J. A. (2009). Cellular origins of beta-cell regeneration: a legacy view of historical controversies. *J. Intern. Med.* **266**, 325-338.
Haumaitre, C., Barbacci, E., Jenny, M., Ott, M. O., Gradwohl, G. and Cereghini, S. (2005). Lack of TCF2/vHNF1 in mice leads to pancreas agenesis. *Proc. Natl. Acad. Sci. USA* **102**, 1490-1495.
Homo-Delarche, F. and Drexhage, H. A. (2004). Immune cells, pancreas development, regeneration and type 1 diabetes. *Trends Immunol.* **25**, 222-229.
Kawaguchi, Y., Cooper, B., Gannon, M., Ray, M., MacDonald, R. J. and Wright, C. V. (2002). The role of the transcriptional regulator Ptf1a in converting intestinal to pancreatic progenitors. *Nat. Genet.* **32**, 128-134.
Kopinke, D., Brailsford, M., Shea, J. E., Leavitt, R., Scaife, C. L. and Murtaugh, L. C. (2011). Lineage tracing reveals the dynamic contribution of Hes1+ cells to the developing and adult pancreas. *Development* **138**, 431-441.
Kopp, J. L., Dubois, C. L., Schaffer, A. E., Hao, E., Shih, H. P., Seymour, P. A., Ma, J. and Sander, M. (2011). Sox9+ ductal cells are multipotent progenitors throughout development but do not produce new endocrine cells in the normal or injured adult pancreas. *Development* **138**, 653-665.
Long, Q., Shelton, K. D., Lindner, J., Jones, J. R. and Magnuson, M. A. (2004). Efficient DNA cassette exchange in mouse embryonic stem cells by staggered positive-negative selection. *Genesis* **39**, 256-262.

Masui, T., Long, Q., Beres, T. M., Magnuson, M. A. and MacDonald, R. J. (2007). Early pancreatic development requires the vertebrate Suppressor of Hairless (RBPJ) in the PTF1 bHLH complex. *Genes Dev.* **21**, 2629-2643.
Minami, K., Okuno, M., Miyawaki, K., Okumachi, A., Ishizaki, K., Oyama, K., Kawaguchi, M., Ishizuka, N., Iwanaga, T. and Seino, S. (2005). Lineage tracing and characterization of insulin-secreting cells generated from adult pancreatic acinar cells. *Proc. Natl. Acad. Sci. USA* **102**, 15116-15121.
Orci, L., Thorens, B., Ravazzola, M. and Lodish, H. F. (1989). Localization of the pancreatic cell glucose transporter to specific plasma membrane domains. *Science* **245**, 295-297.
Pan, F. C. and Wright, C. (2011). Pancreas organogenesis: from bud to plexus to gland. *Dev. Dyn.* **240**, 530-565.
Porat, S., Weinberg-Corem, N., Tornovsky-Babaey, S., Schyr-Ben-Haroush, R., Hija, A., Stolovich-Rain, M., Dadon, D., Granot, Z., Ben-Hur, V., White, P. et al. (2011). Control of pancreatic β cell regeneration by glucose metabolism. *Cell Metab.* **13**, 440-449.
Rovira, M., Scott, S. G., Liss, A. S., Jensen, J., Thayer, S. P. and Leach, S. D. (2010). Isolation and characterization of centroacinar/terminal ductal progenitor cells in adult mouse pancreas. *Proc. Natl. Acad. Sci. USA* **107**, 75-80.
Schaffer, A. E., Freude, K. K., Nelson, S. B. and Sander, M. (2010). Nkx6 transcription factors and Ptf1a function as antagonistic lineage determinants in multipotent pancreatic progenitors. *Dev. Cell* **18**, 1022-1029.
Seymour, P. A., Freude, K. K., Tran, M. N., Mayes, E. E., Jensen, J., Kist, R., Scherer, G. and Sander, M. (2007). SOX9 is required for maintenance of the pancreatic progenitor cell pool. *Proc. Natl. Acad. Sci. USA* **104**, 1865-1870.
Solar, M., Cardalda, C., Houbracken, I., Martín, M., Maestro, M. A., De Medts, N., Xu, X., Grau, V., Heimberg, H., Bouwens, L. et al. (2009). Pancreatic exocrine duct cells give rise to insulin-producing beta cells during embryogenesis but not after birth. *Dev. Cell* **17**, 849-860.
Soriano, P. (1999). Generalized lacZ expression with the ROSA26 Cre reporter strain. *Nat. Genet.* **21**, 70-71.
Srinivas, S., Watanabe, T., Lin, C. S., William, C. M., Tanabe, Y., Jessell, T. M. and Costantini, F. (2001). Cre reporter strains produced by targeted insertion of EYFP and ECFP into the ROSA26 locus. *BMC Dev. Biol.* **1**, 4.
Tessem, J. S., Jensen, J. N., Pelli, H., Dai, X. M., Zong, X. H., Stanley, E. R., Jensen, J. and DeGregori, J. (2008). Critical roles for macrophages in islet angiogenesis and maintenance during pancreatic degeneration. *Diabetes* **57**, 1605-1617.
Thorel, F., Népote, V., Avril, I., Kohno, K., Desgraz, R., Chera, S. and Herrera, P. L. (2010). Conversion of adult pancreatic alpha-cells to beta-cells after extreme beta-cell loss. *Nature* **464**, 1149-1154.
Villasenor, A., Chong, D. C., Henkemeyer, M. and Cleaver, O. (2010). Epithelial dynamics of pancreatic branching morphogenesis. *Development* **137**, 4295-4305.
Wang, A. Y., Ehrhardt, A., Xu, H. and Kay, M. A. (2007). Adenovirus transduction is required for the correction of diabetes using Pdx-1 or Neurogenin-3 in the liver. *Mol. Ther.* **15**, 255-263.
Wang, S., Jensen, J. N., Seymour, P. A., Hsu, W., Dor, Y., Sander, M., Magnuson, M. A., Serup, P. and Gu, G. (2009). Sustained Neurog3 expression in hormone-expressing islet cells is required for endocrine maturation and function. *Proc. Natl. Acad. Sci. USA* **106**, 9715-9720.
Xu, X., D'Hoker, J., Stangé, G., Bonné, S., De Leu, N., Xiao, X., Van de Casteele, M., Mellitzer, G., Ling, Z., Pipeleers, D. et al. (2008). Beta cells can be generated from endogenous progenitors in injured adult mouse pancreas. *Cell* **132**, 197-207.
Zhou, Q., Law, A. C., Rajagopal, J., Anderson, W. J., Gray, P. A. and Melton, D. A. (2007). A multipotent progenitor domain guides pancreatic organogenesis. *Dev. Cell* **13**, 103-114.
Zhou, Q., Brown, J., Kanarek, A., Rajagopal, J. and Melton, D. A. (2008). In vivo reprogramming of adult pancreatic exocrine cells to beta-cells. *Nature* **455**, 627-632.

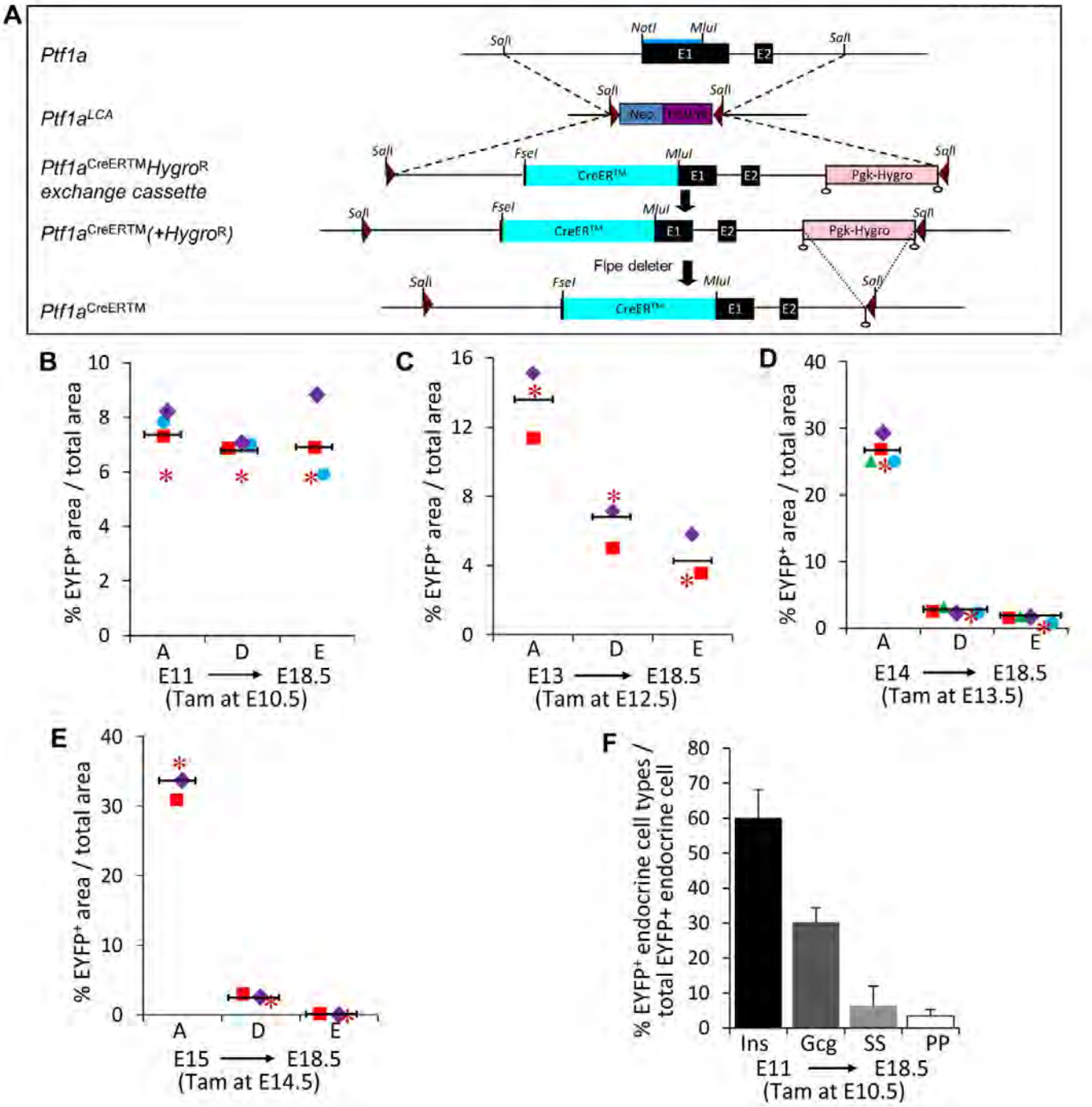

Fig. S1. Lineage tracing of *Ptf1a*-expressing cells using the novel *Ptf1a*^{CreERTM} allele. (A) Schematic representation of *Ptf1a*^{CreER} knock-in generation via recombinase-mediated cassette exchange (RMCE). A *Ptf1a*^{CreERTM}*Hygro*^{R}cassette exchange vector was constructed by inserting a 4105 bp fragment of *Ptf1a* into a plasmid containing two inversely oriented *LoxP* sites, and a 5′UTR *Not*I site was changed to *Fse*I. DNA encoding CreER^{TM} (a gift from Andrew McMahon, Harvard) was then inserted between this *Fse*I and a natural *Mlu*I site in *Ptf1a* exon 1. A *pgk*-driven *hygromycin* resistance gene (*Hygro*^{R}), flanked by tandem FRT sites, was inserted at the 3′ end of the exchange vector for positive selection during RMCE. RMCE was as previously described (Long et al., 2004). An embryonic stem (ES) cell clone 5D12 containing the *Ptf1a*^{LCA} (Burlison et al., 2008) was electroporated with the *Ptf1a*^{CreERTM}*Hygro*^{R} exchange vector and a Cre vector. Clones surviving hygromycin/gancyclovir selection were screened using PCR (primers sequences available upon request). Chimeric mice derived from injecting clone 5D12:1D7 ES cells into C57BL/6J blastocysts were bred with C57BL/6J mice to derive heterozygotes bearing *Ptf1a*^{CreERTM}*Hygro*^{R}. (B-E) The *HygroR* cassette was removed by *FLPe* deleter mice (provided by Susan Dymecki, Harvard). Scatter plots showing the percentage of cells in each pancreatic compartment expressing Eyfp after Tam injection at E10.5 (B; *n*=4), E12.5 (C; *n*=3), E13.5 (D; *n*=5), and E14.5 (E; *n*=3). Each point represents a single pancreas. (F) Ptf1a-expressing cells at E11 contribute equally to all endocrine cell types; *n*=3. A, acinar; D, duct; E, endocrine.

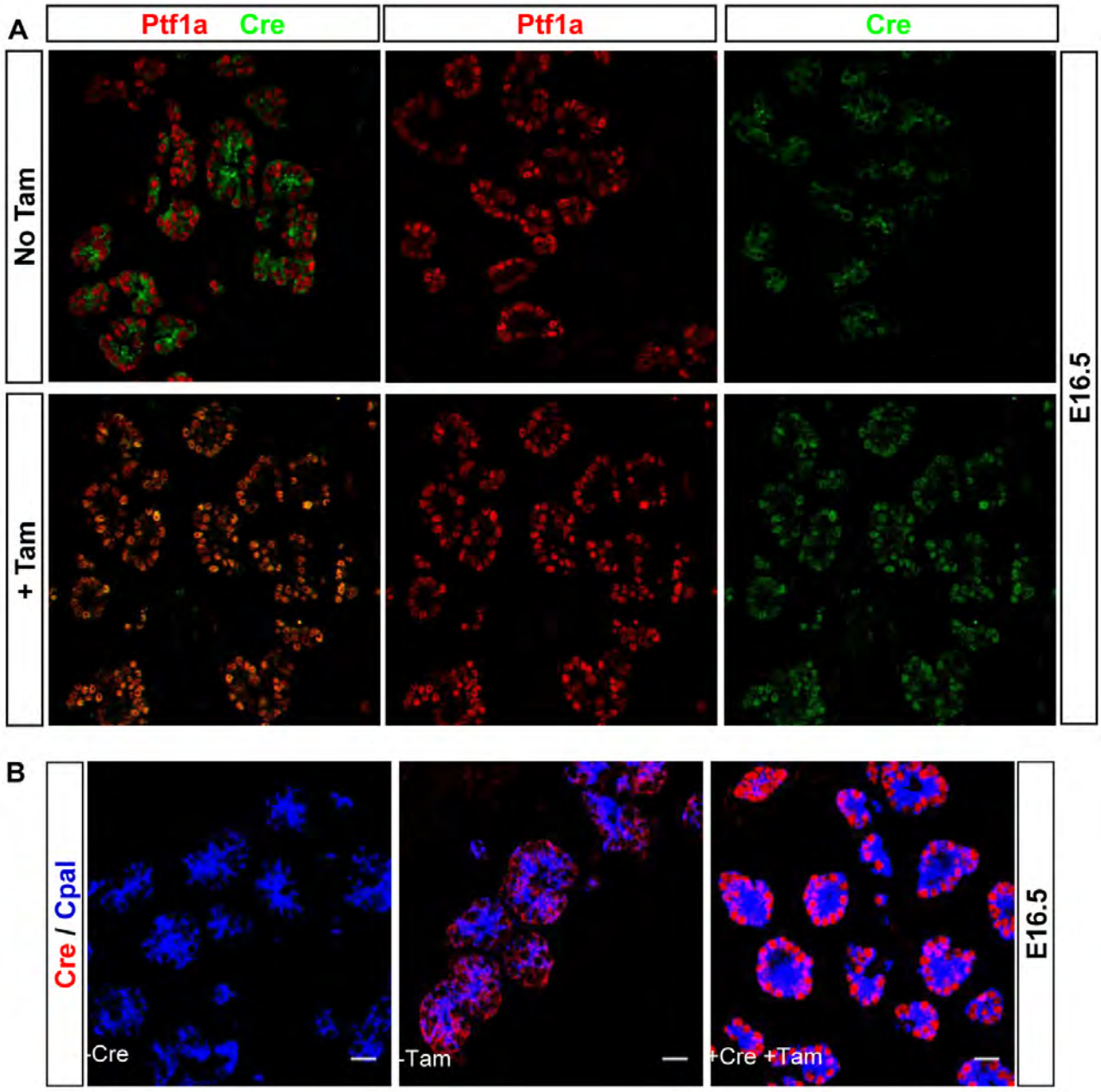

Fig. S2. Cre production recapitulate endogenous Ptf1a production. (**A**) Cre protein is located in the cytoplasm of Ptf1a^{+} cells in the absence of tamoxifen at E16.5 (upper panel); tamoxifen treatment resulted in nuclear translocation of Cre in Ptf1a^{+} cells (lower panel). (**B**) Cre protein was not detected in wild-type E16.5 CpaI^{+} cells, and tamoxifen treatment caused nuclear localization of Cre in CpaI^{+} cells. Scale bar: 50 μm.

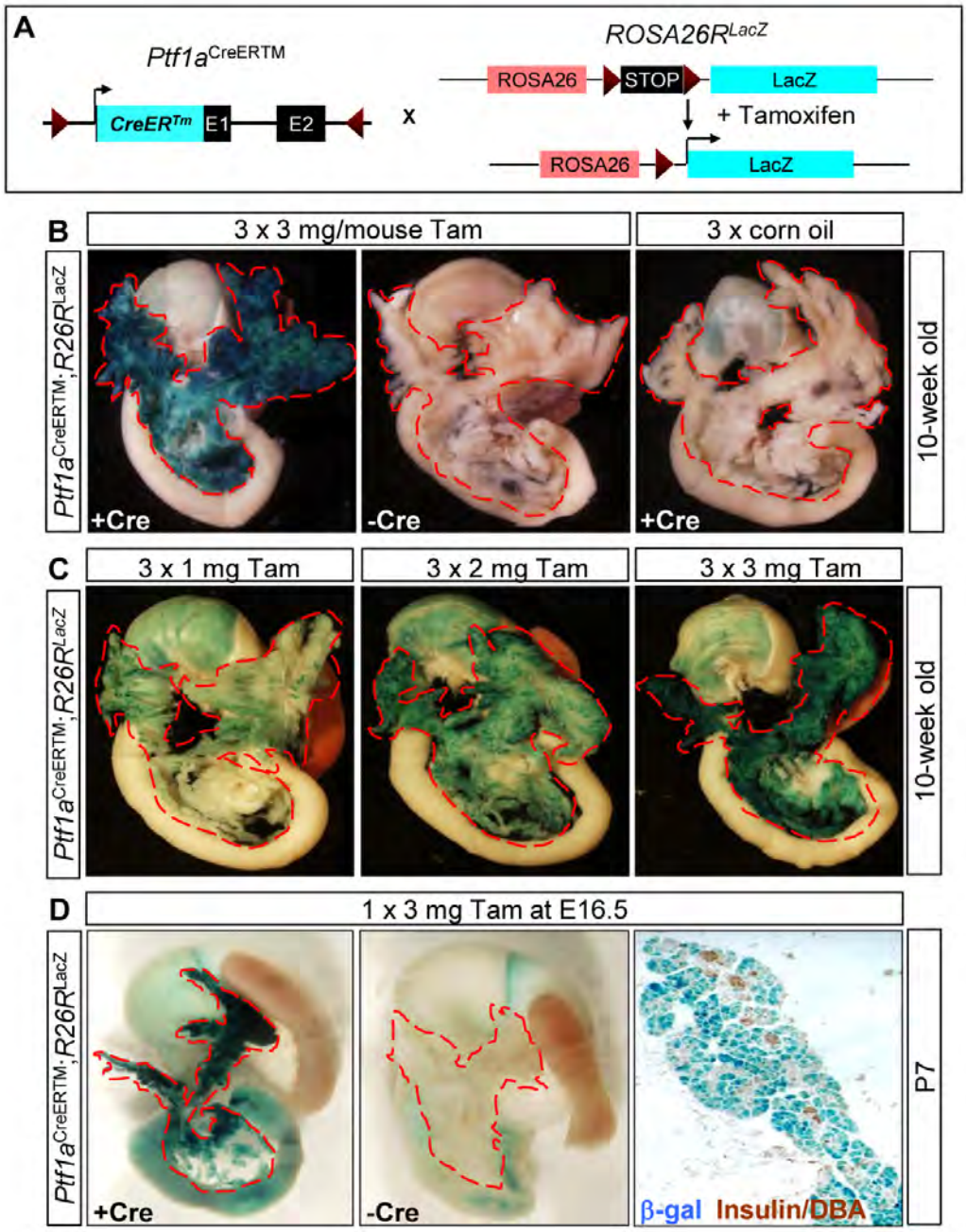

Fig. S3. *Ptf1a*$^{\text{CreERTM}}$-induced recombination at the *ROSA26R*$^{\text{lacZ}}$ allele is Tam and Tam-dosage dependent. (**A**) Schematic presentation of *Ptf1a*$^{\text{CreER}}$-mediated recombination at the *Rosa26*$^{\text{Eyfp}}$ locus only in the presence of Tam. (**B**) Whole-mount β-gal-stained adult gut tissues showed that β-gal staining was found in the pancreas only in the presence of Tam (left panel), but not in corn-oil injected control (right panel), indicating the absence of leakiness. (**C**) There was a Tam-dosage-dependent increase (from 3 to 9 mg) in the β-gal^{+} cell numbers in the pancreas. (**D**) Efficient embryonic labeling at E16.5 after a single dose 3 mg Tam injection (left panel). β-gal staining was mainly found in acinar cells. β-gal staining was not found in the pancreas of mice that did not carry the *Ptf1a*$^{\text{CreERTM}}$ allele (B, middle panel; D, middle panel).

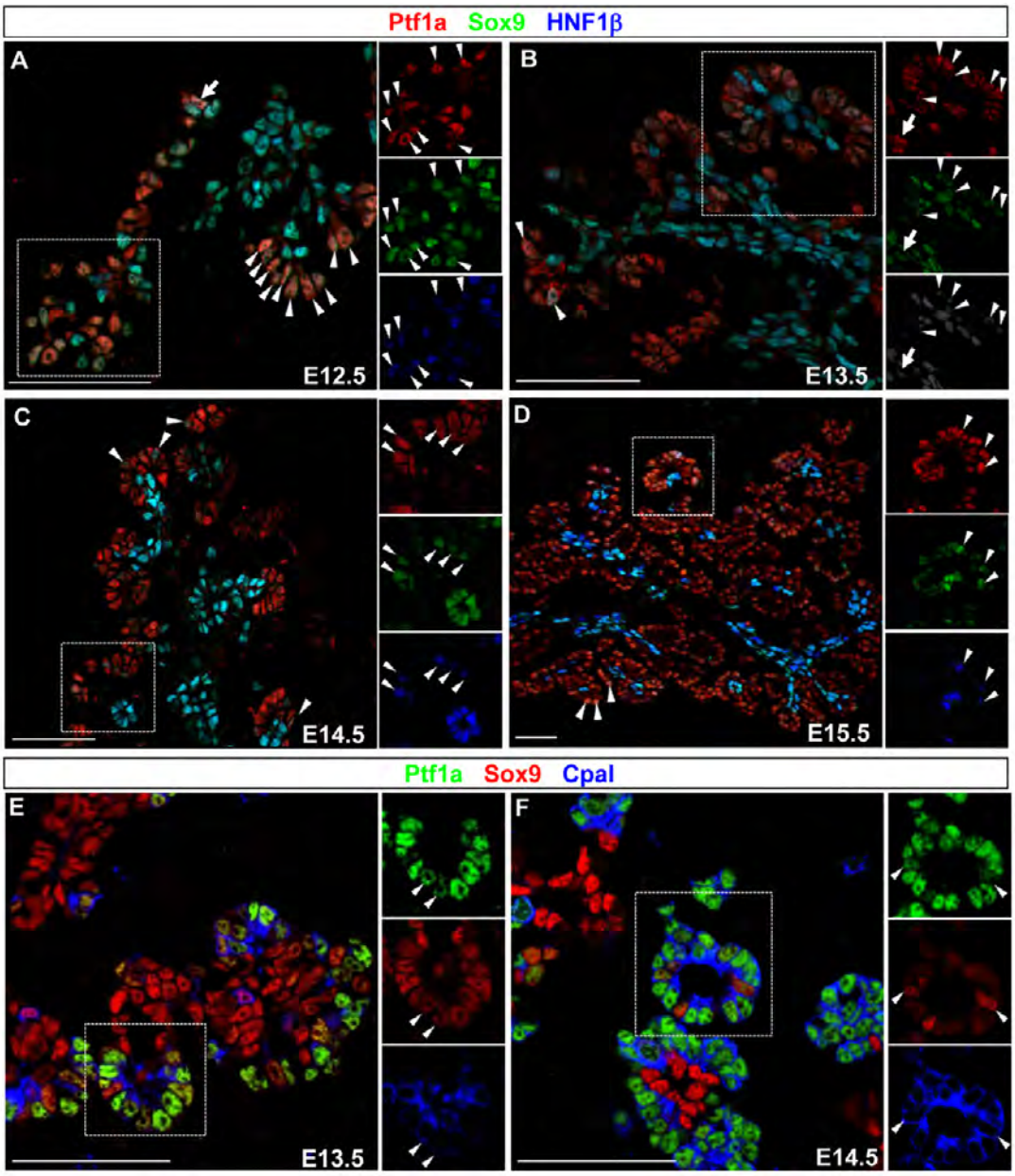

Fig. S4. Distribution of Ptf1a^{+}Sox9^{+}Hnf1β^{+} tip MPCs during the 2° transition. Immunolabeling analysis of Ptf1a, Sox9 and Hnf1β at (**A**) E12.5, (**B**) E13.5, (**C**) E14.5 and (**D**) E15.5 shows the distribution and decreasing numbers of Ptf1a^{+}Sox9^{+}Hnf1β^{+} tip MPCs (arrowhead and arrow) in both intra-tip and tip-trunk interface region. A definite intra-tip location is defined by the location at or near the most distal tip region of the pancreatic epithelium, contact with adjacent pancreatic mesenchyme, and importantly the absence of any cells positive for trunk markers (Sox9^{HI}Hnf1β^{+}) next to that cell's location, from analysis of all of the adjacent sections (arrowhead). 'Tip MPCs' that are located at the tip-trunk interface are defined by proximity to the Sox9^{HI}Hnf1β^{+} trunk cells (arrow). The Ptf1a^{+}Sox9^{+} tip MPCs are also CpaI^{+} (arrowhead) at (**E**) E13.5 and (**F**) E14.5. Scale bar: 50 μm.

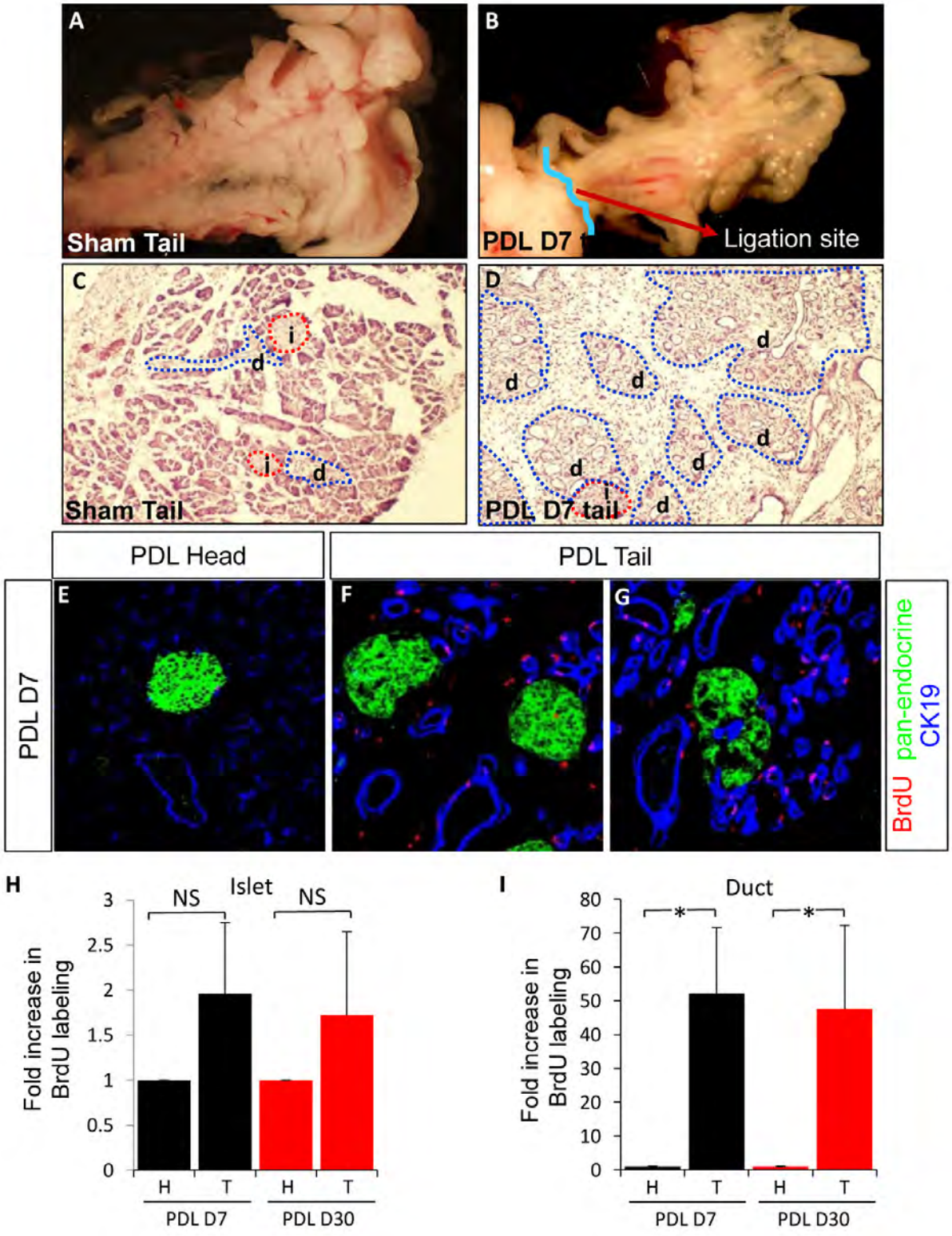

Fig. S5. PDL induces dramatic increased in proliferation in the remodeling ducts. (**A**,**B**) Gross morphological appearance of PDL tail at post-PDL D7 (B) compared to sham tail (A). (**C**,**D**) Sections of sham tail (C) and PDL tail (D) stained with Hematoxylin and Eosin (H&E). (**E-I**) Significant increased BrdU incorporation in the ducts of PDL D7 and D30 tail (F,G,I) compared with PDL head (E,I) indicate active proliferation of remodeling ducts. No significant changes in BrdU labeling in islet cells between PDL head and tail tissues (H). *P<0.005. d, ducts; I, islet; NS, not significant.

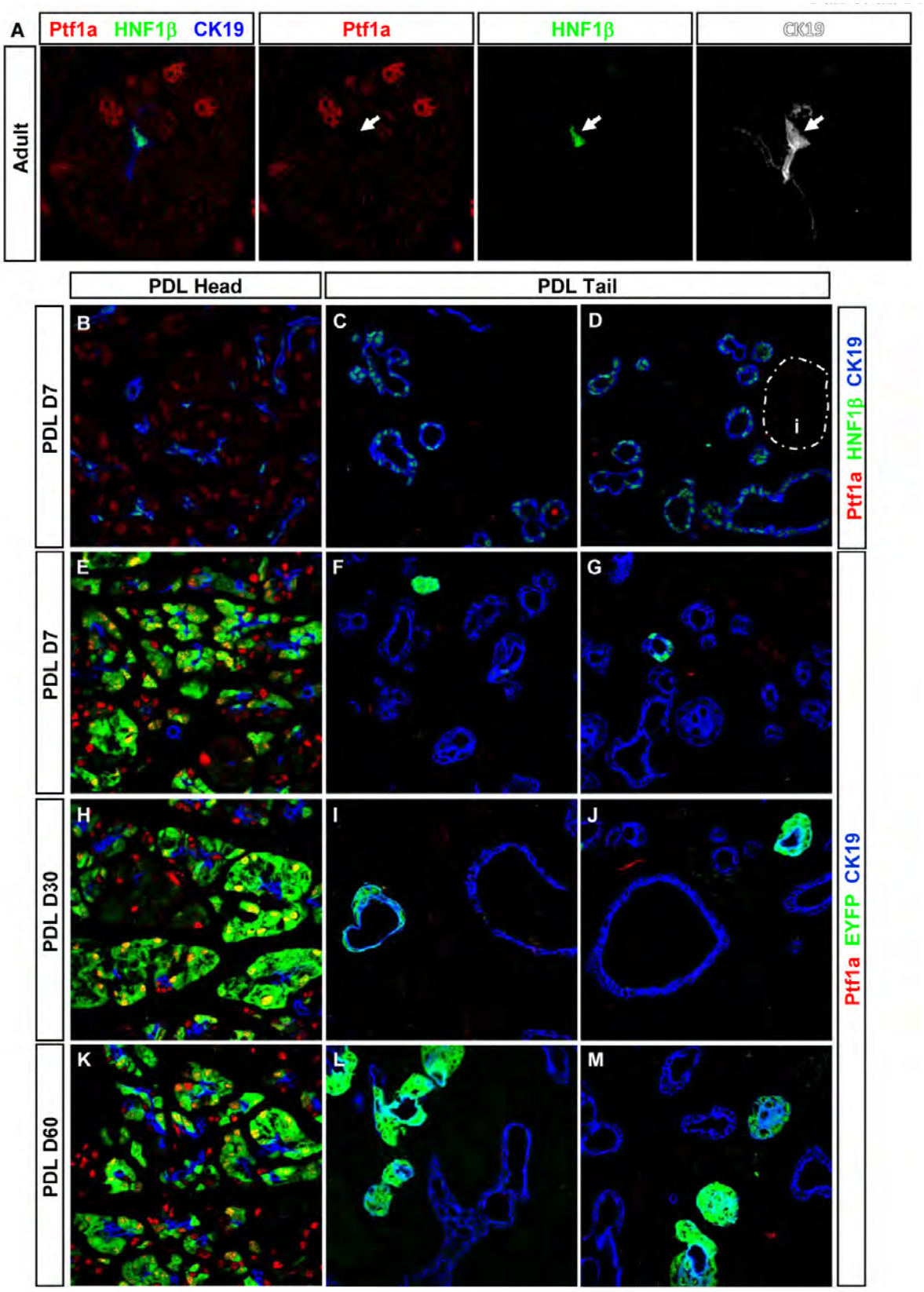

Fig. S6. Ptf1a production in mature adult pancreas and PDL-injured pancreas. (**A**) Ptf1a protein is not detected in Hnf1β^{+}Ck19^{+} CACs. Ptf1a protein is only detected in acinar cells, but not in Hnf1β^{+}Ck19^{+} duct cells in both PDL head and tail tissues at PDL (**B-G**) D7, (**H-J**) D30 and (**K-M**) D60. i, islet.

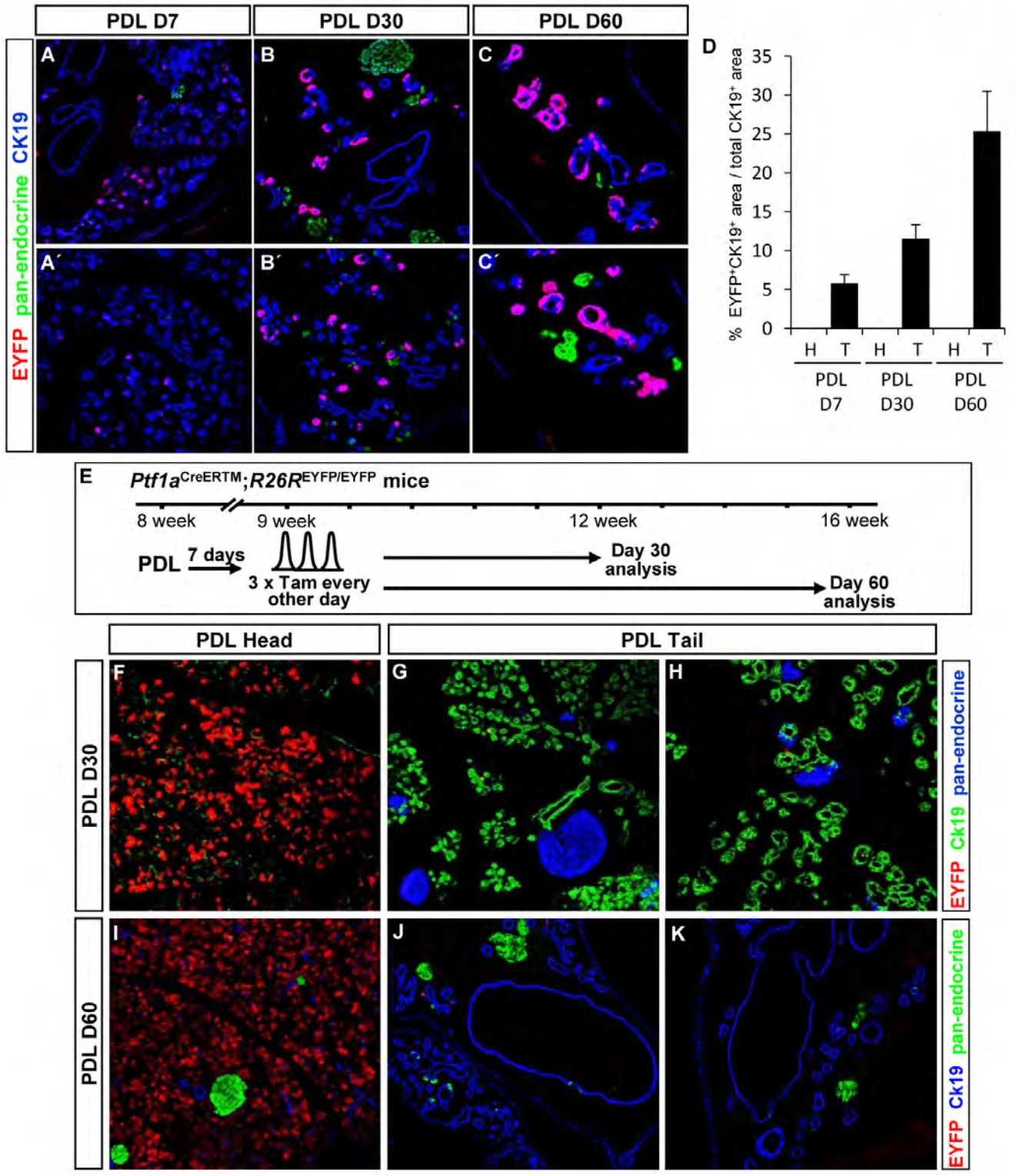

Fig. S7. *Ptf1a* lineage-labeled duct cells were derived from acinar-to-ductal transdifferentiation, and not direct activation of *Ptf1a* expression in the ducts post-PDL. (**A-C′**) *Ptf1a*-lineage labeled (Eyfp^{+}Ck19^{+}) ducts in PDL tail at PDL (A,A′) D7, (B,B′) D30, and (C,C′) D60. (**D**) Quantitation analysis of percentage of Ptf1a-derived duct cells over total Ck19^{+} duct cells. (**E**) Schematic of post-PDL tamoxifen-treatment lineage-tracing analysis. Labeling efficiency in acinar cells remained high in PDL head tissue when tamoxifen was administrated post PDL at PDL (**F**) D30 and (**I**) D60. Very rare *Ptf1a*-derived Ck19^{+} duct cells were found at PDL (**G**,**H**) D30 and (**J**,**K**) D60 when tamoxifen was injected at post-PDL D7.

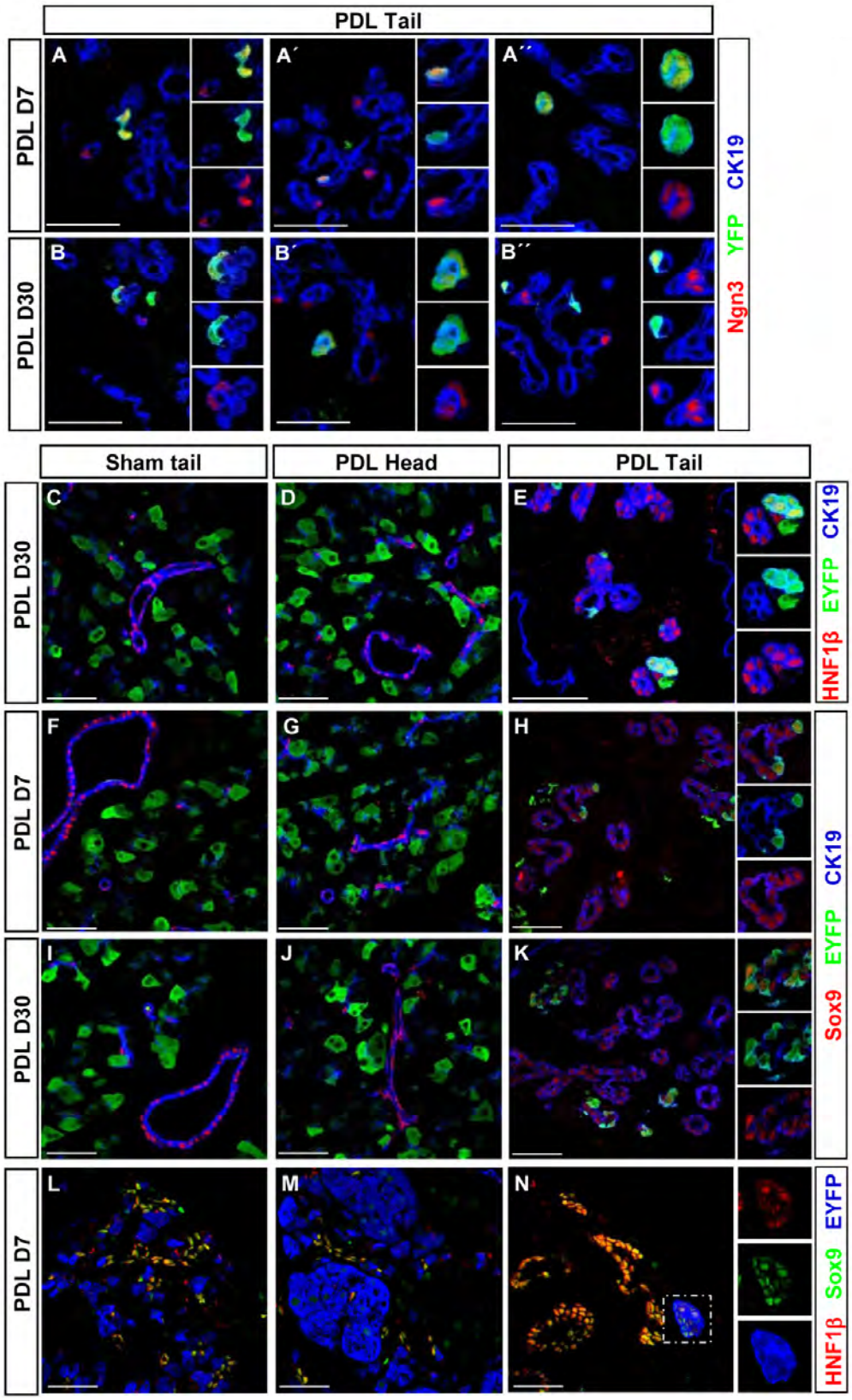

Fig. S8. PDL induces acinar-to-ductal transdifferentiation and activates of Ngn3 protein production in duct cells. (**A-B′**) Additional examples of Ptf1a-lineage-labeled Ngn3^{+}Ck19^{+} duct cells at post-PDL D7 (A-A′) and D30 (B-B′). (**C-N**) Ptf1a^{+} acini gave rise to long-lived Hnf1β^{+} (E) and Sox9^{+} (H,K) duct cells in PDL tail at post-PDL D7 and D30, but not in sham tail (C,F,I) or PDL head (D,G,J). The Sox9^{+}Hnf1β^{+} duct cells are Eyfp^{-} in sham tail (L) or PDL head (M). Most of the Ptf1a^{+} acinar-derived duct cells at PDL D7 are Sox9^{+}Hnf1β^{+} (N). Scale bar: 50 μm.

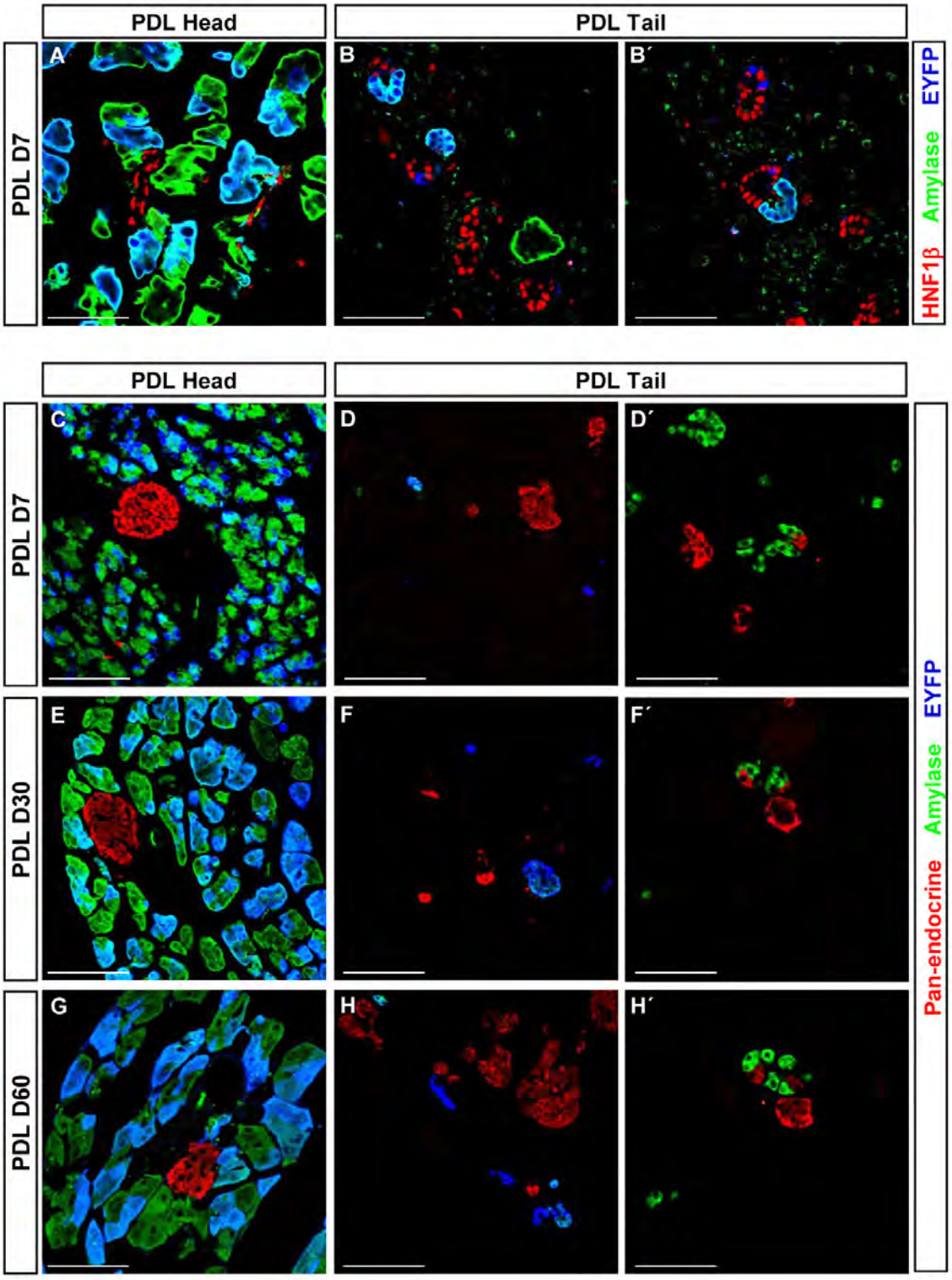

Fig. S9. PDL did not induce direct acinar-to-endocrine transdifferentiation. (**A-B′**) Hnf1β^{+} duct cells did not express amylase at PDL D7 in both head (A) and tail (B,B′), suggesting that acinar enzymes were downregulated before the activation of multipotency factors, such as Hnf1β. (**C-H′**) Amylase was only found in acini in PDL head at PDL D7 (C), D30 (E) and D60 (G). No Amylase^{+}hormone^{+} transitional cell state was found in PDL tail post-PDL D7 (D,D′), D30 (F,F′) and D60 (H,H′), suggesting that Ptf1a-lineage-derived endocrine cells are not a result of rapid, direct acinar transdifferentiation, but stepwise acinar-to-duct-to-endocrine reprogramming.

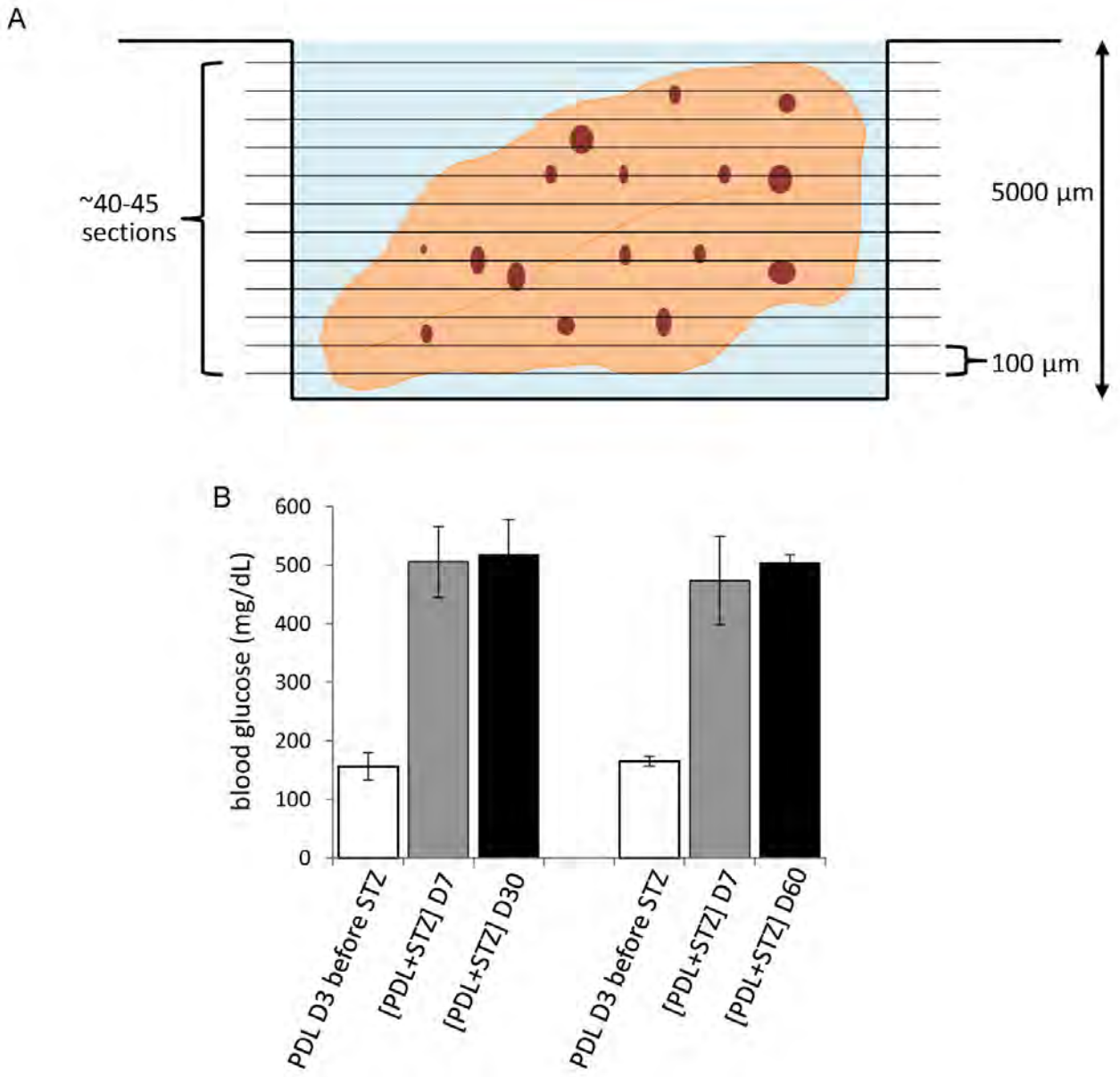

Fig. S10. Strategy for tissue collection and quantitation analysis. Sham tail and PDL tail were embedded in OCT for cryosectioning. (**A**) The whole tissue block was sectioned, we examined ~40-45 sections, taken at 100 µm distance, and stained with a cocktail of endocrine hormones (including insulin, glucagon, somatostatin and pancreatic polypeptide). The pictures were taken at 10´ magnification to include all the hormone$^+$ areas. The islet areas were measured using NIH ImageJ (v. 1.4.3.76) software. (**B**) PDL+STZ treated mice remained hyperglycemic at PDL+STZ D30 and D60. While there is a significant increase in Ptf1a-lineage-derived insulin$^+$ β-cells, the small number of β-cells generated in this transdifferentiation process is therefore insufficient to improve overall glucose homeostasis.

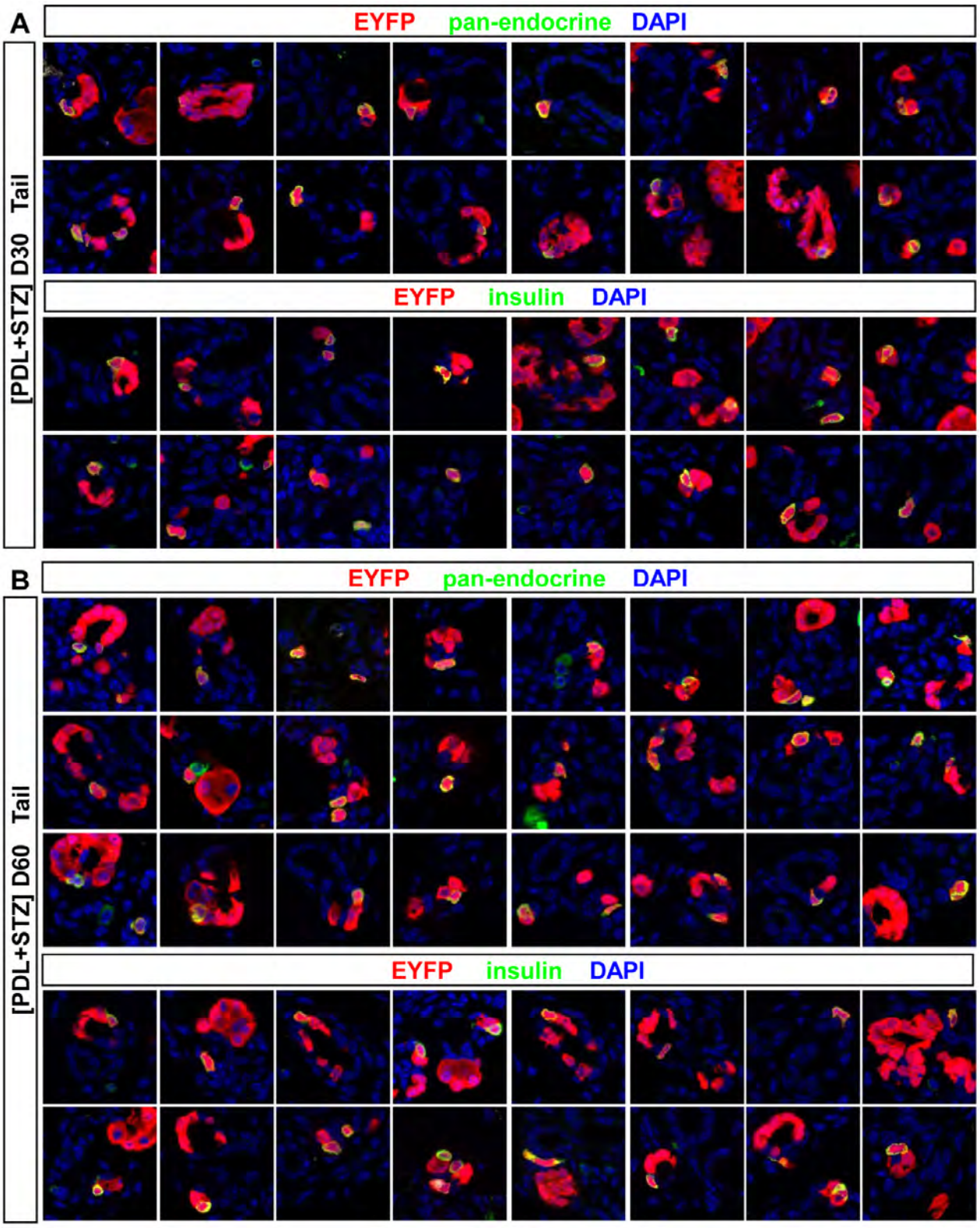

Fig. S11. *Ptf1a* lineage-labeled endocrine/β-cells. Additional examples of *Ptf1a*-lineage-labeled endocrine-hormone$^+$ cells (upper panel) and insulin$^+$ cells (lower panel) at [PDL+STZ] D30 (**A**) and [PDL+STZ] D60 (**B**).

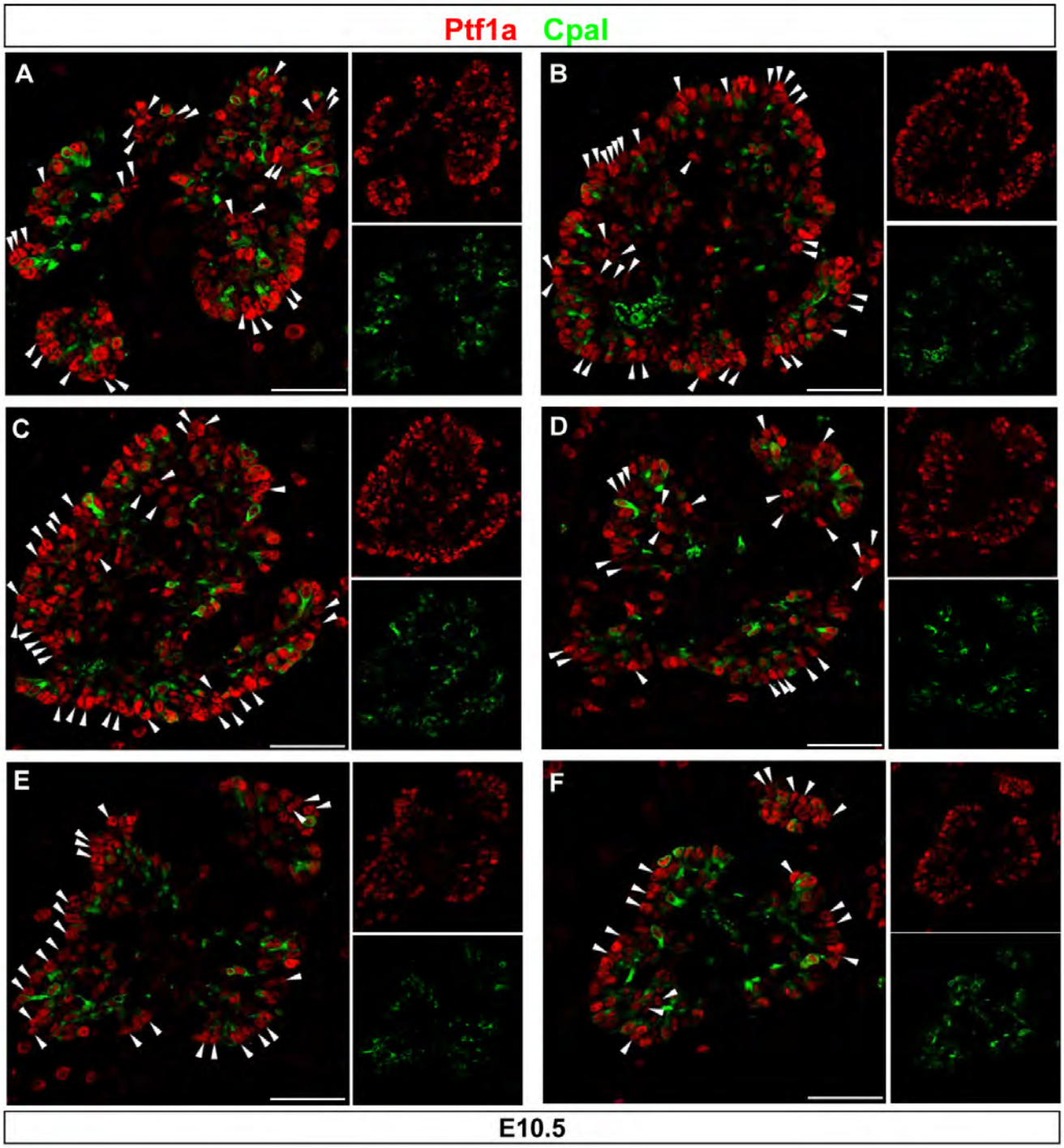

Fig. S12. Numerous Ptf1a^{+} cells do not co-express CpaI at E10.5. (**A-F**) Immunolabeling analysis of Ptf1a and CpaI from different regions of E10.5 dorsal pancreas bud shows that the Ptf1a^{+}CpaI^{-} cells (arrowhead) were frequently found at this stage, suggesting CpaI may only marks a fraction of MPC populations. Scale bar: 50 μm.

Table S1. Antibodies

Primary antibodies				
Antigen	**Species**	**Dilution**	**Staining type**	**Source**
Ptf1a	Rabbit	1:1000	TSA	BCBC
Ptf1a	Guinea pig	1:500	IF	Jane Johnson (UTSW)
Hnf1β	Goat	1:500	TSA	Santa Cruz
Sox9	Rabbit	1:1000	IF	Chemicon
Ngn3	Guinea Pig	1:2000	TSA	M. Sander (UCSD)
GFP	Rabbit	1:500 1:1000	IF TSA	Clontech
GFP	Chicken	1:500	IF	Aves
Insulin	Guinea Pig	1:1000	IF	Linco
Insulin-A	Goat	1:250	IF	Santa Cruz
Glucagon	Guinea Pig	1:1000	IF	Linco
Glucagon	Rabbit	1:1000	IF	Linco
Somatostatin	Goat	1:1000	IF	Santa Cruz
Pancreatic polypeptide	Guinea Pig	1:1000	IF	Linco
CpaI	Goat	1:250	IF	BD Bioscience
E-cadherin	Mouse	1:500	IF	BD Bioscience
BrdU	Mouse	1:500	IF	BD Pharmingen
Ck19	Rabbit	1:2000	IF	B. Stanger (U. Penn)
Dba	Biotinylated	1:250	IF	Vector Laboratories
Synaptophysin	Rabbit	1:1000	TSA	DakoCytomation
Cre	Guinea Pig	1:2000	TSA	C. Wright (Vanderbilt)

Secondary antibodies			
Antigen	**Conjugation**	**Dilution**	**Source**
Rabbit/guinea pig/ goat/mouse/chicken	Cy3	1:300	Jackson ImmunoResearch
Rabbit/guinea pig/ goat/mouse/chicken	Cy2	1:300	Jackson ImmunoResearch
Rabbit/guinea pig/goat/mouse	Cy5	1:300	Jackson ImmunoResearch
Rabbit/guinea pig/ goat/mouse/chicken	Biotinylated	1:1000	Vector Laboratories